University of Maribor
Faculty of Energy Technology

Journal of ENERGY TECHNOLOGY

Volume 8 / Issue 4
DECEMBER 2015
www.fe.um.si/en/jet.html

Journal of ENERGY TECHNOLOGY

VOLUME 8 / Issue 4

Revija Journal of Energy Technology (JET) je indeksirana v bazI INSPEC©.
The Journal of Energy Technology (JET) is indexed and abstracted in database INSPEC©.

JOURNAL OF ENERGY TECHNOLOGY

Izhajanje revije / PUBLISHING

Revija izhaja štirikrat letno v nakladi 150 izvodov. Članki so dostopni na spletni strani revije - www.fe.um.si/si/jet.html / The journal is published four times a year. Articles are available at the journal's home page - www.fe.um.si/en/jet.html.
Cena posameznega izvoda revije (brez DDV) / Price per issue (VAT not included in price): 50,00 EUR
Informacije o naročninah / Subscription information: http://www.fe.um.si/en/jet/subscriptions.html

Lektoriranje / LANGUAGE EDITING

Terry T. JACKSON

Oblikovanje in tisk / DESIGN AND PRINT

Fotografika, Boštjan Colarič s.p.

Naslovna fotografija / COVER PHOTOGRAPH

Jurij AVSEC

Oblikovanje znaka revije / JOURNAL AND LOGO DESIGN

Andrej PREDIN

Ustanovni urednik / FOUNDING EDITOR

Andrej PREDIN

Izdajanje revije JET finančno podpira Javna agencija za raziskovalno dejavnost Republike Slovenije iz sredstev državnega proračuna iz naslova razpisa za sofinanciranje domačih znanstvenih periodičnih publikacij / The Journal of Energy Technology is co-financed by the Slovenian Research Agency.

Spoštovani bralci revije Journal of energy technology (JET)

Vodikove tehnologije in metanolove tehnologije predstavljajo enega ključnih dejavnikov pri načrtovanju sodobnih energetskih naprav. Vodik kot energent se uporablja pri nekaterih tipih vojaških podmornic, avtomobilih, raketni tehniki. Načrtujejo se tudi sistemi soproizvodnje toplotne in električne energije za procese ogrevanja, hlajenja … V ta namen nekatera velika energetska podjetja, kot so Fronius, Panasonic, Vailland in Viessmann, razvijajo sisteme ogrevanja z elektrolizo in gorivnimi celicami. Slednje bi lahko uporabili za pogon računalnikov, ur, transportnih sredstev in sistemov za soproizvodnjo električne ter toplotne energije. Skeptiki opozarjajo na težave, ki jih vodikove tehnologije še vedno imajo, na primer na transport in shranjevanje.

Od leta 2015 je v serijski proizvodnji prvi avtomobil Toyota Mirai, ki je na tržišču Severne Amerike postal prava uspešnica; avtomobil je bil razprodan. Na nemško tržišče naj bi avtomobili prišli v tem letu.

Najbolj pomemben dejavnik za razmah vodikovih tehnologij je proizvodnja poceni vodika. Trenutna proizvodnja bazira na pretvorbi ogljikovodikov. Elektrolizni postopki omogočajo pridobivanje vodika iz vode in so zelo dragi. V svetu so v sklepni fazi razvoja termokemični postopki pridobivanja vodika s pomočjo toplotne energije in majhnega deleža električne energije. Tudi v Sloveniji imamo polnilnico vodika, in sicer v Lescah, obeta pa se izgradnja v Velenju. Srčno upam na velik razmah vodikovih tehnologij, tudi zaradi globalnih ekoloških problemov.

Jurij AVSEC
odgovorni urednik revije JET

Dear Readers of the Journal of Energy Technology (JET)

Hydrogen technologies and methanol technologies represent one of the key factors in the design of modern energy installations. As an energy carrier, hydrogen is already used in some types of military submarines, cars, trains, and rockets. Systems of combined heat and power processes of heating and cooling are planned. For this purpose, some large energy companies, including Fronius, Panasonic, and Vailland and Viessmann, have developed heating systems with electrolysis and fuel cells. Fuel cells could be used to power computers, clocks, transport systems, and systems for the cogeneration of electricity and heat. Skeptics point to the problems that hydrogen technologies still have, such as transportation and storage.

Starting last year, the first hydrogen car in regular production, the Toyota Mirai, has been on sale, primarily in North America. On the German market, such cars should also be released this year.

The most important factor for the growth of hydrogen technologies is the production of cheap hydrogen. Current hydrogen production is based on the conversion of hydrocarbons. The electrolysis process enables the production of hydrogen from water; this is very expensive. Research institutes around the world are in the final stages of the development of thermochemical processes production of hydrogen using heat and a small amount of electricity. In Slovenia, the first hydrogen filling station has opened in Lesce. It is hoped that the next hydrogen filling station will be in Velenje. I sincerely hope the great expansion of hydrogen technologies will continue, especially due to global ecological problems.

Jurij AVSEC
Editor-in-chief of JET

Table of Contents / Kazalo

Determination of local brittle zones at the crack front in the HAZ of welded joint /

Določitev krhkih področij na fronti razpoke v TVP zvarnega spoja

Zdravko Praunseis, Marko Mlakar, Sonja Novak 11

The application of nanomechanics in energy technologies /

Uporaba nanomehanike v energetskih tehnologijah

Jurij Avsec, Urška Novosel 23

On the isochronicity of periodic solutions at a centre manifold /

O izohronosti periodičnih rešitev na centralni mnogoterosti

Brigita Ferčec, Matej Mencinger 43

Design of the ventilation and air-conditioning system in an office building /

Načrtovanje sistema prezračevanja in klimatizacije v poslovni stavbi

Franc Rihl 57

Institut of Energy Technology 70

Instructions for authors 73

JET Journal of Energy Technology

JET Volume 8 (2015) p.p. 11-22
Issue 4, December 2015
Typology of article 1.01
www.fe.um.si/en/jet.html

DETERMINATION OF LOCAL BRITTLE ZONES AT THE CRACK FRONT IN THE HAZ OF WELDED JOINT

DOLOČITEV KRHKIH PODROČIJ NA FRONTI RAZPOKE V TVP ZVARNEGA SPOJA

Zdravko Praunseis[✉], Marko Mlakar[1], Sonja Novak[2]

Keywords: steel welds, heat-affected zone, fracture toughness, crack front

Abstract

Welded joints are the weakest link in the construction of steel structures. The brittlest part of a multi-pass welded joint is the heat-affected zone, where brittle fractures of the structure often appear.

In this article, examination of the whole heat-affected zone of high strength multipass X welded joints was performed. All microstructures and the local brittle zones' sizes at the crack tip front were precisely determined.

Povzetek

Zvarni spoji so pri gradnji energetskih komponent najšibkejši člen jeklene konstrukcije. Najbolj krhko področje večvarkovnega zvarnega spoja je toplotno vplivano področje, kjer se najpogosteje pojavi krhki zlom konstrukcije.

✉ Corresponding author: Zdravko Praunseis, PhD, Faculty of Energy Technology, University of Maribor, Tel.: +386 31 743 753, Fax: +386 7 620 2222, Mailing address: Hočevarjev trg 1, Krško, Slovenia, E-mail address: zdravko.praunseis@um.si

[1] University of Maribor, Faculty of Energy Technology, Hočevarjev trg 1, Krško, Slovenia
[2] University of Maribor, Faculty of Energy Technology, Department Velenje, Koroška 62a, Velenje, Slovenia

V članku je obravnavano celotno toplotno vplivano področje visokotrdnostnega večvarkovnega X zvarnega spoja. Natančno so določene vse krhke mikrostrukture in velikosti lokalno krhki področij ob fronti utrujenostne razpoke.

1 INTRODUCTION

The crack tip opening displacement (CTOD) test has become a common method of measuring the fracture toughness of steel welds. Nevertheless, the commonly used fracture mechanics testing standards, including the CTOD testing standard such as BS 5762, *[2]*, assume the use of metals with a high degree of homogeneity, although this is not explicitly stressed. As already mentioned, in reality, welded joints have typical macroscopic heterogeneity and residual stresses as a result of welding. In order to clarify the applicability of the common testing methods, a basis of knowledge taking the above heterogeneity into account must be established in addition to the standards. Recently, some activities have been conducted for establishing the CTOD testing procedure of steel welds, and some recommended practices/guidelines for CTOD tests of welds have been published.

It is widely understood that the fracture toughness is considerably affected by the shape of the crack front of the fracture toughness specimen, *[6-8]*. Therefore, in the common fracture toughness specimen, attention is carefully paid to realize a straight crack front perpendicular to the plate surface. However, in the welded joint, it is sometimes very difficult to obtain a straight crack front of the fatigue pre-crack due to the existence of weld residual stresses. In order to avoid the confusion due to the irregularity of the crack front and to realize the reproducibility, the current standards require that as a straight crack front as possible be achieved, *[1]*.

2 SECTIONING PROCEDURE TECHNIQUE

In order to achieve a uniform fatigue crack shape which meets the standard requirements, some treatments, i.e. residual stress relieving treatment, have to be applied to notched specimens of welded joints. A different method for relieving residual stresses is to impose a local plastic strain to the region suffering from residual stresses; the following techniques, *[1, 6-8]*, are currently in use,

- Local compression
- Reverse bending
- The use of a high R-ratio in the cycle and step-wise high R-ratio method
- Both side holes method.

Table 1 gives the summary of the relative merits of the three methods. In the Recommended Procedure proposed by The Welding Institute *[8]*, the mechanical relieving residual stresses by local compression, where a plastic strain of 1% of the specimen thickness, is recommended. Moreover, "the use of reverse bending prior to fatigue precracking as a means of redistributing welding stresses is not recommended", *[8]*. Moreover, "the effect of a high R- ratio on the fracture toughness is not well understood and so until more work has been completed on this technique its use is not generally recommended." However, for very thick section welds, "the use of high R-ratios during fatigue precracking has been found to be successful in obtaining acceptable crack front profiles", *[8]*.

***Table 1**: Characteristics of materials used in stress relieving*

Advantages	Disadvantages
LOCAL COMPRESSION	
– method well published – method in use since 1975 – uses normal fatigue precracking procedures	– requires extra operation – requires high capacity compression rig and tools – toughness may be conservative for some materials – specimen must be flat
REVERS BENDING	
– special equipment not needed – conservative toughness measurements expected – uses conventional fatigue pre-cracking procedures	– requires extra operation – toughness may be significantly lower – little information published
USE OF HIGH R-RATIO	
– no extra operation needed – no extra equipment needed	– required loads and R-ratios in conflict with limits of current standards – little information published – non-conservative assessments of toughness are expected

In the common fracture toughness test, the use of a notch sharpened by a precrack produced by fatigue loading of the test piece is generally required in order to simulate sharp macroscopic defects in the structure and to provide a conservative assessment of toughness. In order to avoid the confusion and to realize the reproducibility, the condition of the fatigue precracking loading must be kept within limits.

After the CTOD test is conducted, both halves (or the half containing the weld metal) of the broken specimen are sectioned and metallurgically examined. The cut into the fracture face is taken just behind but within 2.5 mm, of the fatigue-crack front. The cross section may contain a portion of the fracture surface near one or both surfaces due to fatigue-crack front curvature. Each such portion is not wider than 10% of the specimen thickness. For CTOD specimens that are notched to sample the coarse grain (CG) regions, quantification is as shown in Fig. 1, where the linear fraction of the CGHAZ region sampled by the fatigue crack is calculated. A similar procedure is used for the intercritical coarse grain (IC) and subcritical coarse grain (SC) HAZ areas. Fatigue-crack sampling calculations are made by examining enlarged photographs (3 to 6 times magnification) of the CTOD cross sections.

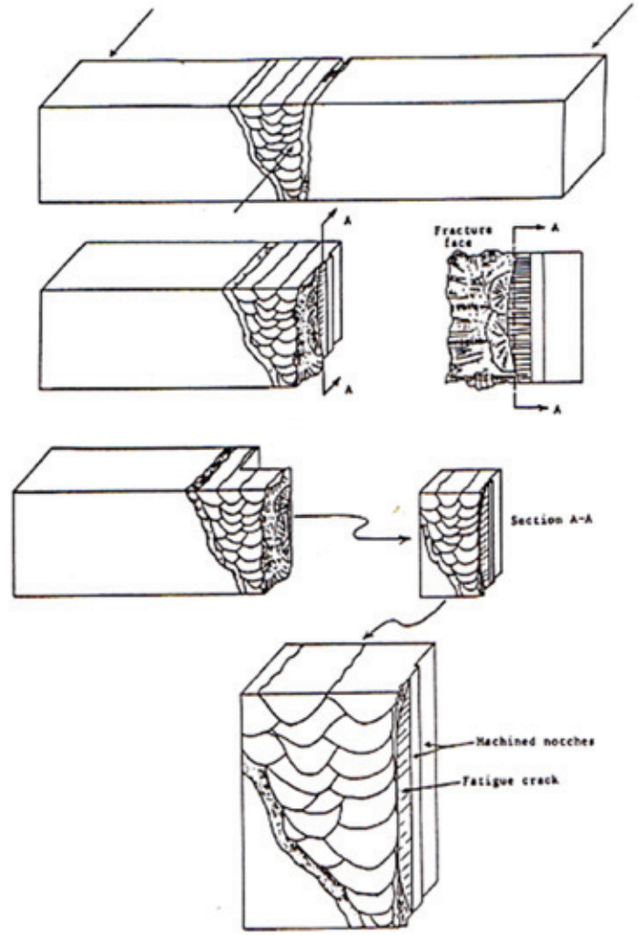

Figure 1: *Sectioning both halves of an HAZ CTOD specimen to calculate CGHAZ percentage*

By using both halves of the broken CTOD specimen and enlarged photographs, fatigue-crack sampling calculations can be made with reasonable accuracy without microscopic examination. Each HAZ specimen should be sectioned to determine the regions of microstructure sampled by the fatigue crack.

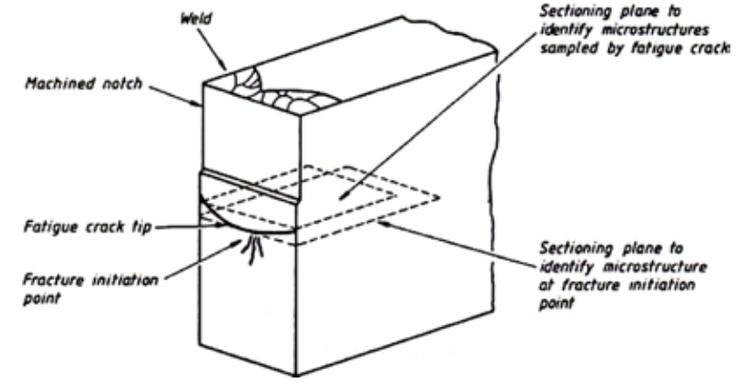

Figure 2: *Example of sections taken from an HAZ, through-thickness notched CTOD specimen to identify microstructures sampled by fatigue crack and at the fracture initiation point*

In the case of through-thickness notched specimens, this is best achieved by sectioning at a small distance behind the fatigue crack tip, so as to include as much of the fatigue crack front as possible (Fig. 2). With surface notched specimens, a similar approach could be used. However, when the region being sampled is small and/or the fatigue crack front is bowed, misleading results may be obtained. For this situation, a better approach is to section as shown in Fig. 3(b), and if necessary, take a series of sections.

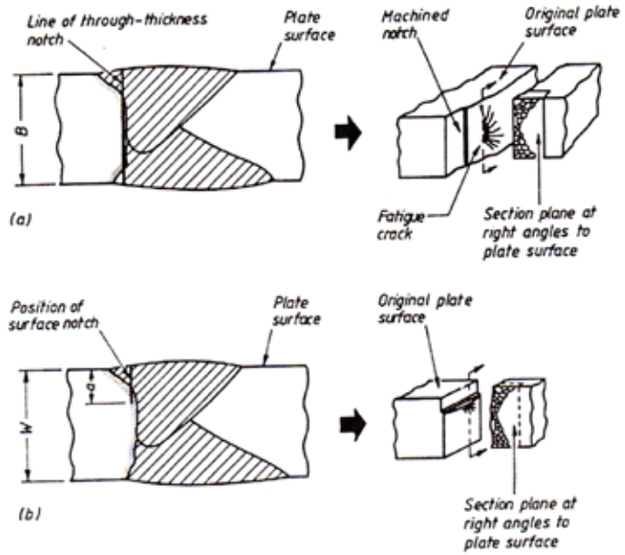

Figure 3: *Example of sectioning techniques for a) through-thickness notched, and -b) surface notched specimens*

It is recommended that similar sectioning procedures be applied to all tests (HAZs and weld metals) carried out to measure the fracture toughness associated with known cracks, *[1]*. By agreement, there is the additional requirement to establish the microstructure at the fracture initiation point; detailed fractography is necessary to determine the microstructure at that point and hence locate the position from which the section has to be taken.

3 EXPERIMENTAL PROCEDURE

Three different types of welded joints were tested for a comparison of mutual mechanical properties. The mechanical properties of the welds made on HSLA steel grade HT50 and HT80 and mild steel were evaluated using standard tensile, *[6]*, Charpy, *[7]*, and CTOD (Crack Tip Opening Displacement) tests, *[8]*. The HAZ specimens were taken from the welded steel plates in the rolling, thickness, and width directions.

The differences in microstructures among material regions influence the mechanical properties, *[6-8]*. Thus, systematic experimental determination of material mechanical properties including fractographical and metallographic investigation of fracture surfaces is necessary.

The chemical composition of the HSLA steel grade HT50 and HT80 and mild steel, with plate thicknesses of 40 mm are given in Table 2. All testing HAZ specimens were taken from the steel plates in the rolling direction (A), the thickness direction (B), and the width direction (C).

The yield strength and tensile strength were obtained using round bar tensile specimens, as shown in Fig. 4. Tensile testing was done at room temperature (20 ºC).

Table 2: *Chemical composition of the HSLA steel grade HT50 and HT80 and mild steel*

Composition (%)	HT50	HT80	Mild steel
C	0.12	0.16	0.28
Si	0.55	0.68	0.52
Mn	0.67	0.75	0.71
P	0.015	0.020	0.011
S	0.002	0.003	0.007
Cr	0.70	0.79	0.05
Ni	0.07	0.09	0.01
Mo	0.042	0.032	0.013
Cu	0.19	0.24	0.62
Al	0.001	0.002	0.001

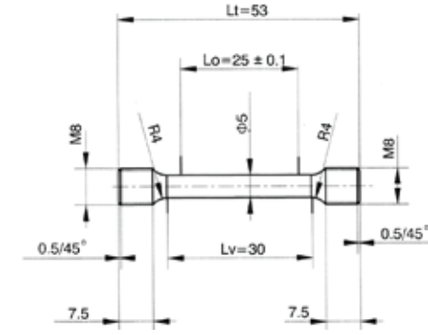

Figure 4: *Tensile round bar specimen B 5 × 25*

Charpy - V testing was used to determine the impact toughness of steel plates. The shape and dimensions of a standard Charpy - V specimen, mechanically notched, are shown in Fig. 5. Testing was performed at -10 ºC. For every test temperature, three specimens were fractured.

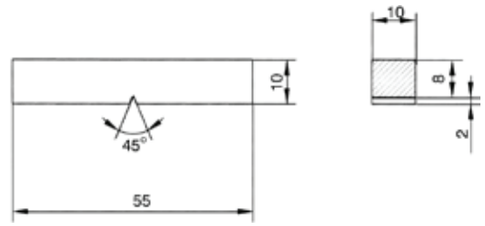

Figure 5: *Shape and dimensions of Charpy – V notch specimen*

CTOD fracture toughness of the welds made on HSLA steel grade HT50 and HT80 and mild steel was evaluated using standard static CTOD test, [4-5]. Specimen loading was carried out with constant crosshead speed v = 0.5 mm/min. The test temperature was -10 ºC according to the recommendation of the OMAE (Offshore Mechanics and Artic Engineering) association. For CTOD testing, the single specimen method was used, *[8]*. To evaluate the fracture toughness of steels, standard fracture mechanics tensile specimens with shallow notches were used, as shown in Fig. 6.

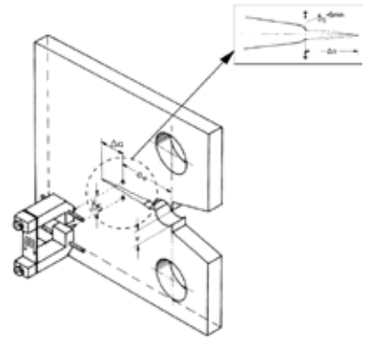

Figure 6: *Direct measurement of CTOD values at the crack tip of fracture mechanics specimen*

For all specimens, the fatigue precracking was carried out with the Step-Wise High R ratio (SHR) method procedure, *[4]*. During the CTOD tests the potential drop technique was used for monitoring stable crack growth, *[5]*. The CTOD values were directly measured with a special clip gauge, *[5]*, on the specimen side surfaces at the fatigue crack tip over a gauge length of 5 mm (see Fig. 6).

4 DISCUSSION OF RESULTS

Mechanical properties of welds made on HSLA steel HT80 and HT50 and mild steel plate in the rolling direction (A), thickness direction (B) and the width direction (C) are presented in Table 3. The basic values of yield strain and tensile strain of testing steels, given in Table 3, were obtained from engineering stress (R) - strain (e) diagrams. It is known that engineering material curves cannot be used for analysis of material deformation characteristics and finite element calculations in the range of high plastic deformations.

Average Charpy-V testing values of three fractured specimens are represented in Table 3.

Table 3: *Mechanical properties of welds made on HSLA steel HT80 and HT50 and mild steel plate in the rolling direction (A), thickness direction (B) and width direction (C)*

Weld-Steel grade	Measured direction	Yield strain (MPa)	Tensile strain (MPa)	CTOD (mm)	Charpy V (J) at –10 ºC
HT50	A	542	591	0.390	47, 68, 71 Av=62
HT80	A	693	830	0.401	69, 78, 64 Av=70
Mild steel	A	452	497	0.423	42, 55, 62 Av=53
HT50	B	501	562	0.240	39, 41, 55 Av=45
HT80	B	657	799	0.253	53, 68, 66 Av=62
Mild steel	B	439	471	0.231	39, 44, 61 Av=48
HT50	C	531	587	0.416	42, 76, 69 Av=62
HT80	C	665	811	0.478	67, 71, 63 Av=67
Mild steel	C	447	478	0.443	40, 51, 65 Av=52

The lowest Charpy toughness was measured in the HAZ specimens taken from the steel plates in the thickness direction (B). The cause for low toughness was the appearance of inconvenient ferritic microstructures with distributed brittle martensite-austenite (M-A) constituents (Fig. 7).

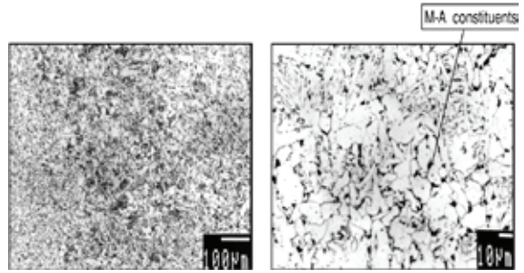

Figure 7: *Ferritic microstructure with distributed brittle M-A constituents along ferrite grain boundaries of HAZ specimen*

The Charpy toughness of HAZ specimens taken from the steel plates in the rolling direction (A) is approximately equal to the Charpy toughness of HAZ specimens taken from the steel plates in the width direction (C).

Directly measured CTOD values of HAZ fracture toughness for each type of steels are summarized in Table 3. The maximal CTOD toughness was measured in the HAZ specimens with the crack tip located in the width direction (C).

In the case of CTOD testing of HAZ specimens with the crack tip located in the thickness direction (B), the lowest CTOD was measured due to the appearance of the first brittle fracture in the mainly ferritic microstructure with carbides (Fe3C), precipitated at the grain boundary (Fig. 8) and the appearance of brittle fracture initiation point, i.e. Al-Si-Mn inclusions (Fig. 9). For the correct identification of a brittle fracture initiation point, it is of utmost importance to apply Energy Disperse X-ray (EDX) analysis to both fracture surfaces. In the opposite case, it could happen that the EDX analysis detects some fictitious brittle fracture initiation point.

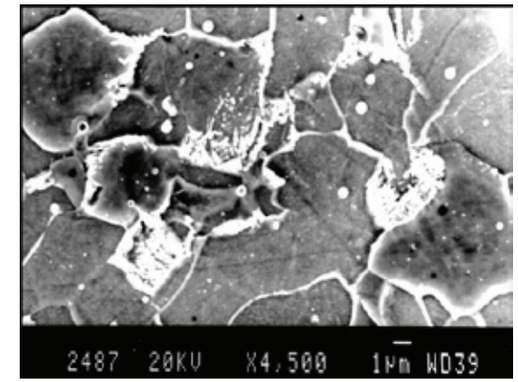

Figure 8: *Mainly ferritic microstructure with carbides (Fe_3C) precipitated at the HAZ grain boundary*

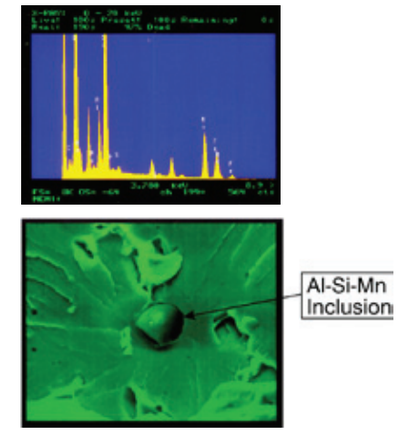

Figure 9: *Appearance and EDX analysis of brittle fracture initiation point, i.e. Al-Si-Mn inclusion in the HAZ specimen*

5 CONCLUSION

Exact evaluation of real material mechanical properties is essential for the safe servicing of energy components. The presence of different HAZ microstructures along pre-crack fatigue fronts has significant effects on the critical crack tip opening displacement (CTOD). This value is the relevant parameter for the safe servicing of modern energy components. The mechanical properties of welds made on of HSLA steels grade HT50 and HT80 and mild steel are the lowest in the thickness direction of the steel plate due to the appearance of carbides (Fe3C) and Al-Si-Mn inclusions in the ferritic microstructure. The mechanical properties of welds made on HSLA steels grade HT50 and HT80 and mild steel are approximately equal in the rolling and in the width directions of the steel plates.

References

[1] **Mlakar, M.:** *Determination of local brittle zones at the crack front in the HAZ of welded joint. Master Thesis,* Faculty of Energy Technology, University of Maribor, Slovenia, 2015

[2] BS 5762, *Methods for crack opening displacement (COD) testing*, The British Standards Institution, London 1979

[3] ASTM E 1152-87, *Standard test method for determining J-R curves*, Annual Book of ASTM Standards, Vol. 03.01, American Society for Testing and Materials, Philadelphia, 1990

[4] ASTM E 1290-91, *Standard test method for crack-tip opening displacement (CTOD) fracture toughness measurement,* American Society for Testing and Materials, Philadelphia, 1991

[5] GKSS Forschungszentrum Geesthacht GMBH, *GKSS-Displacement Gauge Systems for Applications in Fracture Mechanic*

[6] **Praunseis, Z., Toyoda, M., Sundararajan, T.**: *Fracture behaviours of fracture toughness testing specimens with metallurgical heterogeneity along crack front*. Steel res., 71, Vol. 9, Sep. 2000

[7] **Praunseis, Z**., **Sundararajan, T., Toyoda, M., Ohata, M.:** *The influence of soft root on fracture behaviors of high-strength, low-alloyed (HSLA) steel weldments*. Mater. manuf. process., Vol. 16, 2001

[8] **Toyoda, M.:** Fracture toughness evaluation of steel welds, Book of Mechanics, Osaka University, 1989

Acknowledgements

The authors wish to acknowledge the financial support of the Slovenian Foundation of Science and Technology and the Japanese Promotion of Science.

JET Journal of Energy Technology

JET Volume 8 (2015) p.p. 23-41
Issue 4, December 2015
Typology of article 1.01
www.fe.um.si/en/jet.html

THE APPLICATION OF NANOMECHANICS IN ENERGY TECHNOLOGIES

UPORABA NANOMEHANIKE V ENERGESKIH TEHNOLOGIJAH

Jurij Avsec[R], Urška Novosel[1]

Keywords: nanomechanics, nanotechnology, nanomaterials, nanoenergetics

Abstract

Nanotechnologies may be very efficient for improving and optimizing energy technologies. The following will be shown in this paper: nanomaterials are very important in energy technology. Nanofluids and nanostructured materials may be applied in refrigerators, heaters, and similar equipment. In the micro- and nano-regions, the classic laws of mechanics are insufficiently accurate for the calculation of characteristics and properties. In this article, the application of microfluidics and vibration theory in the micro and nano-regions will be shown.

Povzetek

Nanotehnologije so lahko zelo učinkovite za izboljšanje in optimizacijo energetskih procesov. Razvoj nanomaterialov je izjemnega pomena za energetiko. Nanotekočine in nano nanostrukturirani materiali se lahko uporabljajo v hladilnih strojih, grelnikih.... V mikro in nano-področju zakoni klasične termomehanike v mnogih primerih niso dovolj natančni. V ta namen je tudi prikazana problematika v mikrofluidni tehniki in mehanskih nihanjih.

[R] Corresponding author: Prof. Jurij Avsec, University of Maribor, Faculty of Energy Technology, Laboratory for Thermomechanics, Applied Thermal Energy Technologies and Nanotechnologies , Tel.: +386-7-6202217, Fax: +386-2-620-2222, Mailing address: Hočevarjev trg 1, 8270 Krško, Slovenia
E-mail address: jurij.avsec@um.si

[1] University of Maribor, Faculty of Energy Technology, Laboratory for Thermomechanics, Applied Thermal Energy Technologies and Nanotechnologies, Hočevarjev trg 1, SI-8270 Krško, Slovenia

1 INTRODUCTION

Along with the development of increasingly larger devices, many inventors and scientists have attempted to penetrate the secrets of the nanoworld. For centuries, watchmakers were miniaturizing mechanical devices. The discovery of the microscope in the 17th century enabled people to observe microbial, plant, and animal cells. Only in the late 20th century, however, were the technologies of microdevices developed. The size of transistors in integrated circuits is currently 0.18 micrometres, and laboratories are already developing transistors of 10 nanometres. One of the great scientific and technical advancements at the turn of the 21st century is the creation of nanomaterials and nanotechnology. The area that covers all significant problems from that field is called “mechanics” in the broadest sense, which is divided into:

- macromechanics 10^{-4}-10^{-5} m,
- mesomechanics 10^{-5}-10^{-7} m,
- micromechanics 10^{-7}-10^{-8} m,
- nanomechanics: 10^{-8}-10^{-9} m.

Since the atomic level (interatomic distance in a crystal lattice) has an order of one to several Å (10^{-10} m), the nanolevel is restricted to 10^{-9} m.

Nanotechnology currently allows the successful manufacture of micro-electro-mechanical systems (MEMS), nano-electro-mechanical systems (NEMS) and biological micro-electro-mechanical systems (BIO MEMS). Significant among these are microchips, micro sensors, micro mirrors biochips, and nanomaterials.

Micro-electro-mechanical systems are devices with a characteristic length ranging between 1 mm and 1 micrometre and consisting of electric and mechanical components. Microdevices, for example, are smaller than the diameter of a human hair. Nanodevices (NEMS) are devices of even smaller dimensions, containing nanocomponents or devices based on special materials called nanomaterials.

Nanomechanics and micromechanics are becoming even more important in modern industry. Ideas about extremely small aircraft, pumps and other technical devices have become reality today, *[1-9]*. At the same time, unforeseen problems have emerged. If a fluid flows through a pipe with the diameter of a few nanometres or micrometres, thermodynamic and transport properties of the fluid are modelled completely differently due to the high impact of the surface effects. Similarly, the equations of conventional hydromechanics do not apply in the entire area. In addition to temperature and pressure, the significance of the Knudsen number (Kn) is also growing. This number is the ratio of the mean free path length of the molecules to a characteristic length L, *[2-5]*.

The Euler equation for the calculation of flow gives poor results in almost the entire range, from the Navier-Stokes equation at a Knudsen number of 0.1 to the Burnett equation at a Knudsen number of 10. To analyse the molecular free path in micro- and nano-channels, non-equilibrium mechanics and the original Boltzmann equation should be used to be able to calculate hydro-mechanical problems in the entire range of Knudsen numbers.

Nanofluids of exceptional properties are increasingly economically important. In addition to nanofluids, the application of nanopipes with even better properties is also increasing in engineering practice.

Nanotechnology will expand into many areas in the future. Digital data storage with much higher recording densities will be possible as well as analyses of individual cells in cases of serious illnesses as well as the manufacture of ultra-light materials with exceptional properties. The size of nanoparticles and nanowires is nearly the same as the size of biomolecules, such as DNA molecules and proteins. In the future, it will be possible to use nanoparticles in various areas of medicines. Consideration is being given to applying nanoparticles as a suitable probe for small DNA samples or proteins.

2 NANOMATERIALS

Nanomaterials are classified in the next divisions, *[1-3]*:

1) Carbon-based nanomaterials

2) Metallic nano-materials

2) Nanocomposites

3) Metals & alloys

4) Biological nanomaterials

5) Nano-polymers

6) Nano-glasses

7) Nano-ceramics

8) Natural nanoparticles

The term ‘nanofluid’ is envisioned as describing a solid-liquid mixture that consists of nanoparticles and a base liquid; this is one of the new challenges of nano-technology for thermo-sciences. The possible application area of nanofluids is in advanced cooling systems, and in micro/nano electromechanical systems. The investigation of the effective thermal conductivity of liquid with nanoparticles attract much more interest experimentally and theoretically. The effective thermal conductivity of nanoparticle suspension can be much higher than for the fluid without nanoparticles.

The calculation of properties for nanofluids for real substances is possible with the use of classical and statistical mechanics. Classical mechanics has no insight into the microstructure of the substance. Statistical mechanics, in contrast, calculates the properties of a state on the basis of the molecular motions in a space, and on the basis of the intermolecular interactions. The equations obtained by means of classical thermodynamics are empirical and apply only in the region under observation. The main drawback of classical thermodynamics is that it lacks the insight into the substance of microstructures. In contrast to classical mechanics, statistical mechanics calculates the thermomechanical properties of state on the basis of intermolecular and intramolecular interactions between particles in the same system of molecules. It deals with the systems composed of a vast number of particles. Figure 1 and Figure 2 shows the thermal conductivity and viscosity for nanofluids obtained by statistical thermomechanics.

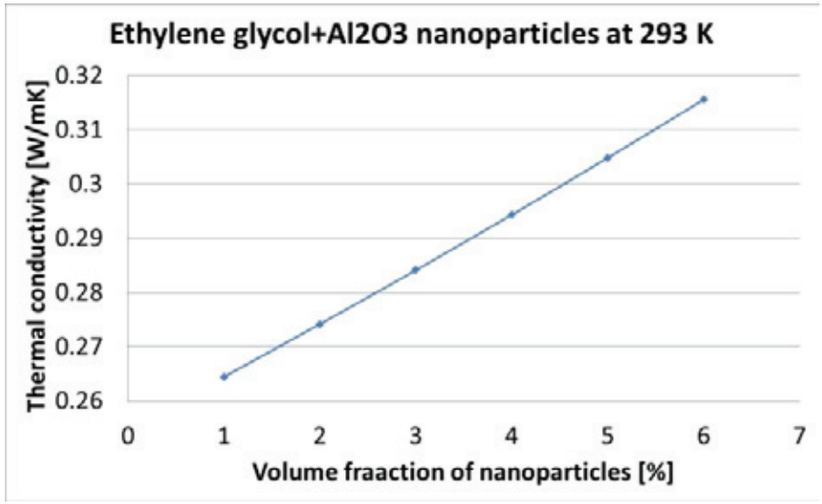

Figure 1: *Thermal conductivity of mixture between ethylene glycol and Al_2O_3 nanoparticles*

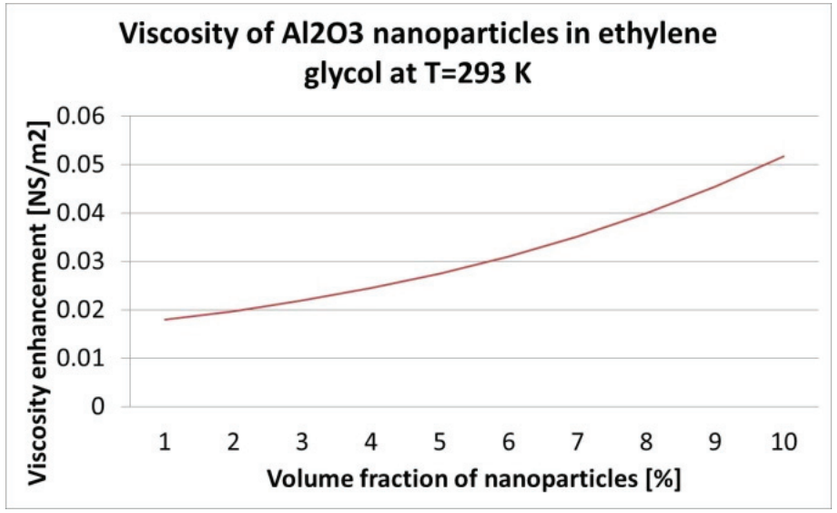

Figure 2: *Thermal conductivity of mixture between ethylene glycol and Al2O3 nanoparticles*

3 MICROFLUIDICS

Fluid flow in channels, minichannels, and microchannels is driven due to the presence of electric fields, magnetic fields or pressure-driven flows and some other effects, *[1]*.

Electrohydrodynamics (EHD), known as electrokinetics, is the theory of the flow of electrically charged fluids. It is the study of the motions of ionised particles or molecules and their interactions with electric fields and the surrounding fluid. For EHD flow, low electrical conducting fluids, such as organic fluids or alcohols, are required, *[2-4].* The electrokinetic flow can be classified into the following types: electrophoresis, electroosmosis, streaming potential and sedimental potential, *[2-5]*.

The fundamental concept for magnetohydrodynamics (MHD) is that magnetic fields can induce currents in a moving conductive fluid, which in turn creates forces on the fluid and also changes the magnetic field itself, *[2].* For MHD flows, highly conductive fluids, such as plasmas, liquid metals, electrolytes and salt water, are needed.

f the flow is transported by pressure differential, the phenomenon is called pressure hydrodynamics (PHD).

Ferrohydrodynamics (FHD) is the theory of magnetic fluid flow.

The term ‘nanofluid’ is envisioned as describing a solid-liquid mixture that consists of nanoparticles and a base liquid; this is one of the new challenges for thermo-sciences provided by nano-technology. The possible application area of nanofluids is in advanced cooling systems, and in micro/nano-electro-mechanical systems. The investigation of the effective thermal conductivity of liquid with nanoparticles has attracted much more interest experimentally and theoretically. The effective thermal conductivity of nanoparticle suspensions can be much higher than for the fluid without nanoparticles.

The calculation of properties for nanofluids for real substances is done using classical and statistical mechanics. Classical mechanics has no insight into the microstructure of the substance. Statistical mechanics, in contrast, calculates the properties of the state on the basis of molecular motions in a space, and on the basis of the intermolecular interactions. The equations obtained by means of classical thermodynamics are empirical and apply only in the region under observation. The main drawback of classical thermodynamics is that it lacks insight into the substance of the microstructure. In contrast to classical mechanics, statistical mechanics calculates the thermomechanical properties of state on the basis of intermolecular and intramolecular interactions between particles in the same system of molecules. It deals with systems composed of a very large number of particles.

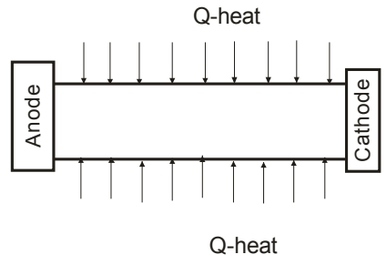

a) Electrokinetic flow

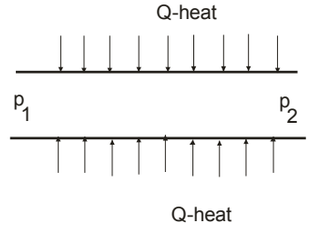

b) Pressure-driven flow

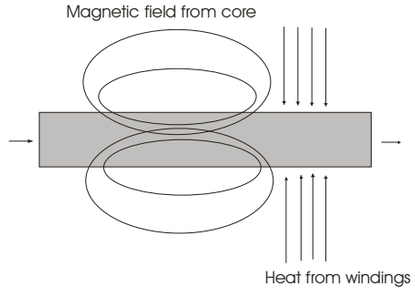

c) Ferrofluid flow

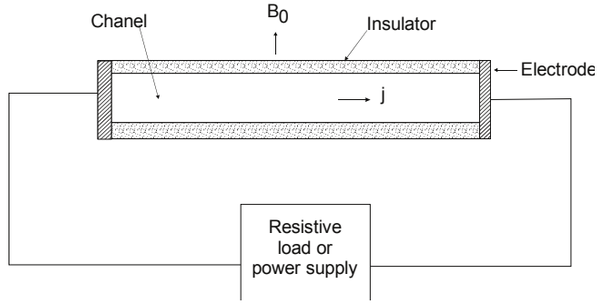

d) MHD flow

Figure 3: *Types of fluid flow*

Consider the MHD flow in rectangular and circular microchannels (Figure 3). The charged surface of a microchannel wall may attract ions of the opposite charge in the surrounding fluid. The general form of the momentum equation for MHD flow is:

$$\rho\frac{\partial\vec{v}}{\partial t}+\rho\vec{v}\nabla\vec{v}=-\nabla p+\nabla\left(\mu\nabla\vec{v}\right)+\vec{i}\times\vec{B}\,, \tag{3.1}$$

where the last term represents the electromagnetic force, and i and B refer to the current density and magnetic field strength, respectively. For steady-state flow in a microchannel at small Reynolds numbers, the transient and inertia terms can be neglected, so Eq. (3.1) is simplified in the next equation:

$$0=-\nabla p+\nabla\left(\mu\nabla\vec{v}\right)+\vec{i}\times\vec{B}\,, \tag{3.2}$$

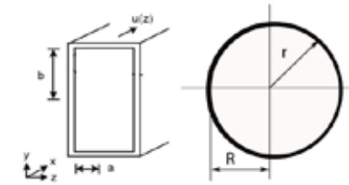

Figure 4: *Rectangular and circular microchannels*

Assuming the fluid velocity, magnetic field and current density are orthogonal, the reduced momentum equation becomes:

$$0=-\frac{dp}{dx}+\mu\frac{d^2u}{dz^2}+i_yB_z \tag{3.3}$$

The terms represent pressure, viscous and electromagnetic forces in the liquid. Using Ohm's Law to express the current density in terms of fluid velocity:

$$\mu\frac{d^2u}{dz^2}+\sigma_eB_z^2u=\frac{dp}{dx}\,, \tag{3.4}$$

where σ_e and B_z refer to the electrical conductivity and magnetic field strength. For fully developed flow in a microchannel, the pressure gradient becomes constant and independent of the magnetic field strength. In terms of the Hartman number, M_H ($M_H=aB_z\sqrt{\sigma_e/\mu}$),

$$\mu\frac{d^2u}{dz^2}-\left(\frac{M_H{}^2\eta}{a^2}\right)u=\frac{dp}{dx} \tag{3.5}$$

Applying the no-slip boundary conditions at z=0 and z=-2a, the analytical solution of Eq. (3.5) becomes:

$$u = -\frac{a^2\left(\frac{dp}{dx}\right)}{M_H{}^2\mu} + \frac{a^2\left(\frac{dp}{dx}\right)}{\left(1+2e^{2M_H}\right)M_H{}^2\mu} e^{\frac{z\cdot M_H}{a}} + \frac{a^2\left(\frac{dp}{dx}\right)e^{2M_H}}{\left(1+2e^{2M_H}\right)M_H{}^2\mu} e^{\frac{-z\cdot M_H}{a}} \quad (3.6)$$

The mean velocity within the microchannel becomes:

$$u_b = \frac{1}{2a}\int_0^{2a} u(z)dz \qquad u_b = \frac{a^2\left(\frac{dp}{dx}\right)(-M_H+Tanh(M_H))}{M_H{}^3\mu}$$

Non-dimensionalizing this result (z^*=z/a, u^*=u/u_b), we obtain the next equation:

$$u^* = \frac{M_H\left(-1+\frac{1}{\left(1+2e^{2M_H}\right)}e^{z^*\cdot M_H}+\frac{e^{2M_H}}{\left(1+2e^{2M_H}\right)}e^{-z^*\cdot M_H}\right)}{(-M_H+Tanh(M_H))} \quad (3.7)$$

Without electromagnetic effects, Equations (3.5-3.7) transform into the following expressions:

$$u(z) = \frac{\left(\frac{dp}{dx}\right)}{2\mu}\left(-2az+z^2\right), u_b = \frac{1}{2a}\int_{-a}^{a} u(z)dz = \frac{a^2\left(\frac{dp}{dx}\right)}{3\mu}, u^* = \frac{3}{2}\left(2-z^*\right)z^* \quad (3.8)$$

For the circular microchannel without electromagnetic forces, the governing equation is

$$\frac{dp}{dx} = \mu\left(\frac{\partial^2 u}{\partial r^2}+\frac{1}{r}\frac{\partial u}{\partial r}\right) \quad (3.9)$$

Solving the differential equation subject to boundary conditions,

$$u = \frac{\left(\frac{dp}{dx}\right)}{4\mu}(r^2-R^2),\ u_b = \frac{1}{\pi R^2}\int_0^R u2\pi\, r\cdot dr = -\frac{\left(\frac{dp}{dx}\right)R^2}{8\mu}\ u^* = 2-2r^{*2} \quad (3.10)$$

If we wish to calculate the velocity profile for MHD flow in a circular channel, we have to solve the following differential equation:

$$\frac{dp}{dx} = \mu\left(\frac{\partial^2 u}{\partial r^2}+\frac{1}{r}\frac{\partial u}{\partial r}\right) - \mu\frac{M_H{}^2}{R^2}u \quad (3.11)$$

The analytical solution of equation (3.11) is slightly more complicated. We have obtained the next solution of the differential equation with the boundary conditions (u(R)=0, u'(0)=0):

$$u[r] = \frac{R^2\left(\frac{dp}{dx}\right)(-\text{BesselI}[0,M]+\text{BesselI}[0,\frac{Mr}{R}])}{M^2\mu\,\text{BesselI}[0,M]} \quad (3.12)$$

$$u_b = \frac{1}{\pi R^2}\int_0^R u2\pi\, r\cdot dr = \frac{R^2\left(\frac{dp}{dx}\right)\text{BesselI}[2,M]}{M^2\mu\,\text{BesselI}[0,M]} \quad (3.13)$$

Previous investigations of the pressure gradient for electro-osmotic liquid flow in microchannels have generally used no-slip conditions, while for gas flow in microchannels, the slip boundary condition is taken into account. Some previous experimental investigations have demonstrated the existence of liquid slip on a microchannel wall, *[2-5]*. In addition, some previous studies were numerically performed considering a slip velocity for a liquid flow in a microchannel made from hydrophobic surfaces, taking into account the electric field and pressure gradient, *[3-5]*. Furthermore, some previous studies numerically predicted a slip velocity for liquid flow in a microchannel made from hydrophobic surfaces, taking into account an imposed electric field and a pressure gradient without heat transfer. On the basis of a slip velocity profile and boundary conditions in liquid microchannel flow, the velocity profile can be determined by

$$u(0) = u_{s1}, u(2a) = u_{s2} \quad (3.14)$$

$$u_{s1} = \beta\frac{\partial u}{\partial z}\Big|_{z=0},\ u_{s2} = \beta\frac{\partial u}{\partial z}\Big|_{z=2a} \quad (3.15)$$

Figures 5-9 show the analytical results for the velocity profile in fluids in dependance of slip conditions, type of microchannel and type of fluid flow.

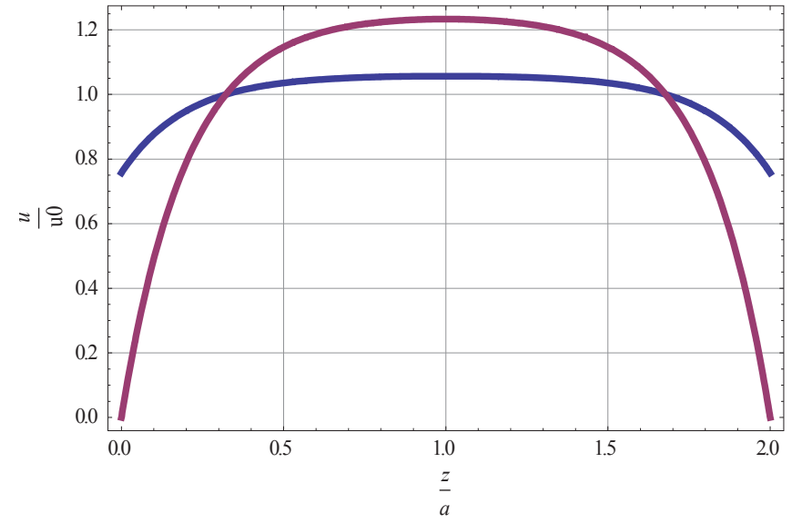

Figure 5: *Velocity profile (a) without slip (red line) and with slip β*=0.5 (blue line) at MH=5 in rectangular minichannel*

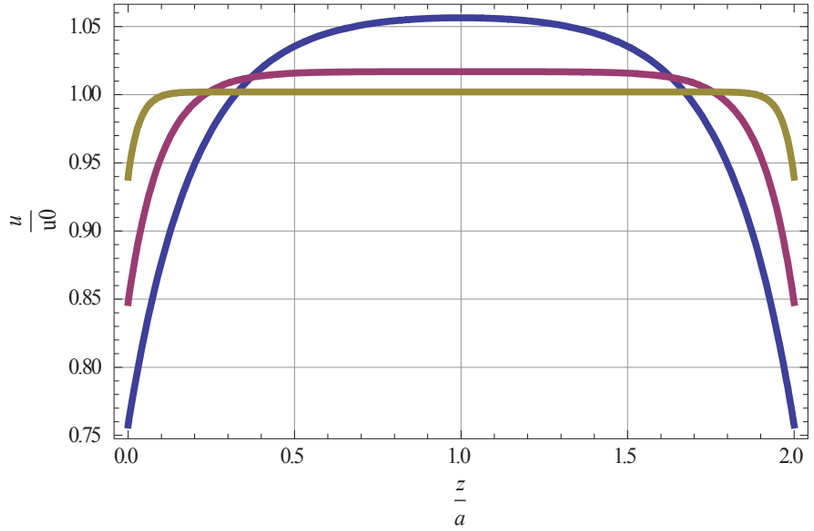

Figure 6: *Velocity profile with slip (β*=0.5) at MH=5 (blue line), MH=10 (red line) and MH=30 (green line) in rectangular minichannel with slip β*=0.5*

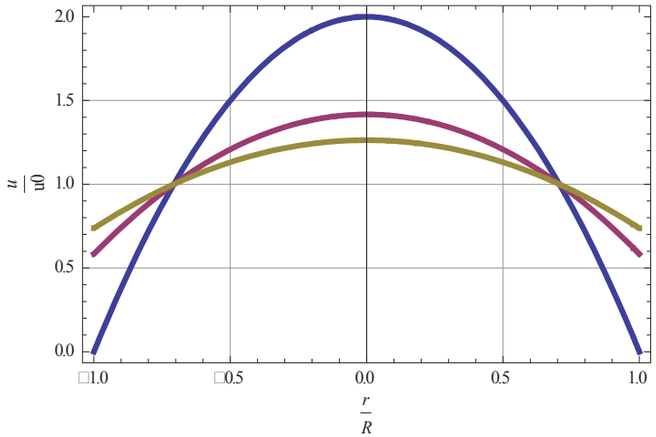

Figure 7: *Velocity profile in a circular microchannel without electromagnetic effects (blue line), with a slip with slip β*=0.35 (red line) and with slip β*=0.7 (green line)*

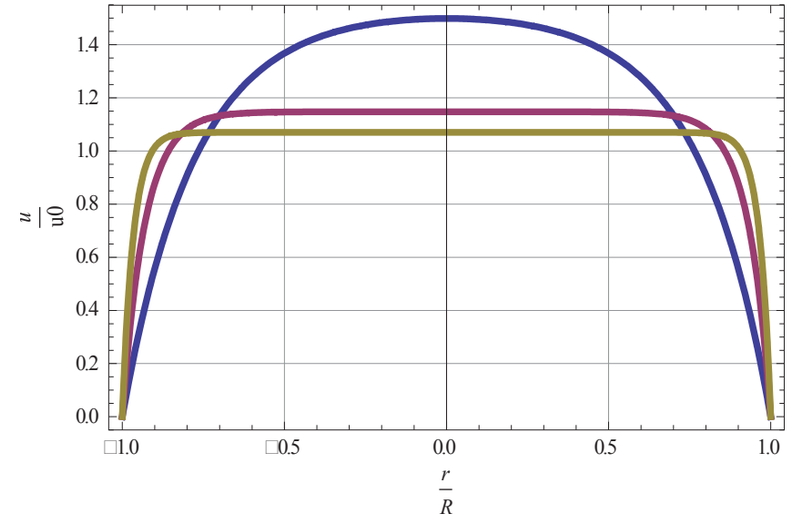

Figure 8: *Velocity profile with slip (β*=0.5) at MH=5 (blue line), MH=10 (red line) and MH=30 (green line) in circular microchannel without slip*

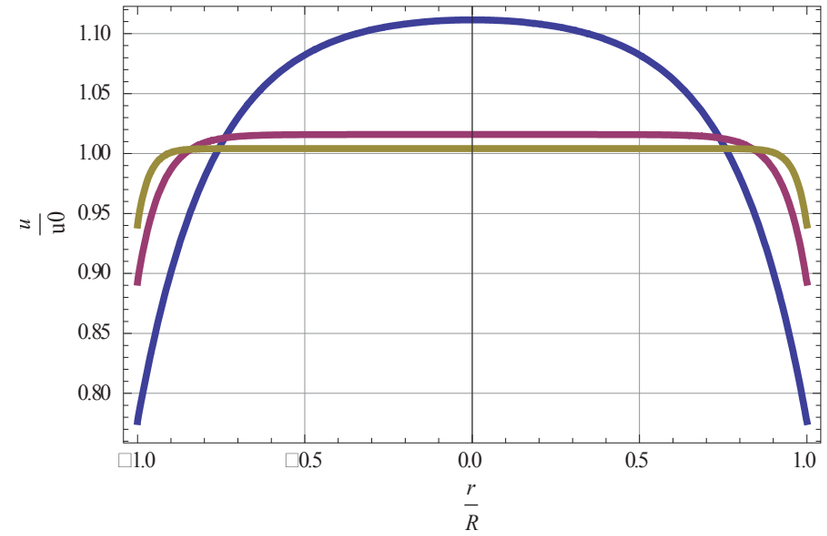

Figure 9: *Velocity profile with slip β*=0.5 at MH=5 (blue line), MH=10 (red line) and MH=30 (green line) in circular microchannel*

4 THE VIBRATIONS OF MICROBEAMS AND NANOBEAMS

The vibrations of beams, microbeams and nanobeams are of vital importance in mechanical engineering. Mechanical machines very frequently operate under diverse temperature conditions. In internal combustion engines, rocket systems, satellites, as well as MEMS and NEMS, conditions are particularly temperature-sensitive. Thermodynamic effects are frequently ignored in research, which may yield completely incorrect results. Literature, *[3]*, shows that even the slightest temperature change leads to significant alteration of the clamped-beam vibration properties. In the present paper the impact of a change in thermodynamic properties, which have to be taken into consideration with major temperature changes, is not neglected. Carbon nanotubes in dependence of the chiral angle can be classified into three types: armchair, zigzag, and chiral. Numerous studies are available on the physical properties of armchair and zigzag carbon nanotubes [14-15]. However, only a limited portion of the literature studied nanotubes in dependence of temperature field. This article develops a model that analyses the frequency of the chiral single-walled carbon nanotubes (SWCNTs) subjected to thermal vibrations by using the Timoshenko beam model, including the effect of rotary inertia and shear deformation. The Timoshenko model has been compared with the Euler model.

Carbon nanotubes can be classified into single wall nanotubes (SWNT) and multi-wall nanotubes (MWNT). On the basis of molecular simulation, many researchers have found that the modulus of elasticity is no longer constant, and is dependent on the diameter of nanotube and thickness of nanotube *[6-16]*. On the basis of molecular dynamics calculation, equations for surface Young modulus and Poisson number for armchair SWNT can be expressed:

$$Y_s = \frac{4\mu K_p}{\sqrt{3}(\lambda + 3\mu)} \tag{4.1}$$

where:

$$\mathrm{v} = \frac{\lambda - \zeta\mu}{\lambda + \zeta\mu},\ \lambda = \frac{7 - \cos(\pi/n)}{34 + 2\cos(\pi/n)},\ \mu = \frac{K_\theta^2}{K_\rho r_0^2} \tag{4.2}$$

The above equations are obtained on the basis of continuous mechanics and molecular simulation, *[6-8]*, where Y_s means surface Young modulus, and v the Poisson number. From Fig. 3.10, we can see that material properties are both temperature and size dependent.

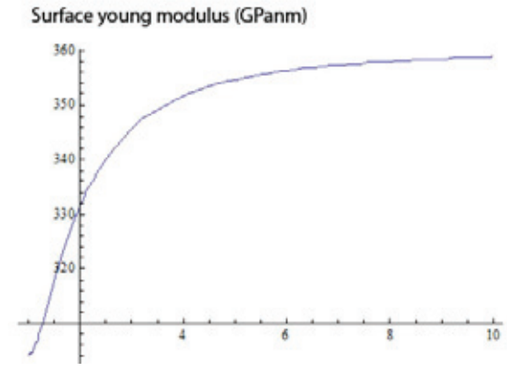

Figure 10: *Young modulus of armchair nanotubes*

The Young modulus of carbon nanotubes and the linear expansion coefficient are also dependent on the temperature field. On the basis of Prakash, *[16]*, a molecular dynamics simulation is obtained and the next relation for modulus of elasticity and linear expansion coefficient α for SWNT:

$$Y_s = Y_s(1 - 0.000075T) \tag{4.3}$$

$$\alpha = \frac{1}{l}\left(\frac{dl}{dT}\right) = \frac{10^{-18}T^2 - 2*10^{-15}*T + 10^{-13}}{10^{-18}T^3 - 10^{-15}T^2 + 10^{-13}T + 3*10^{-8}} \tag{4.4}$$

4.1 Local Euler-Bernoulli beam model under thermal stresses

Let us assume that the support is homogenous, having the same temperature over its entire length. As a result of thermal expansion, an additional axial force F_T occurs:

$$F_T = \alpha\theta EA \tag{4.5}$$

In equation (3.7), α is the linear thermal extension coefficient, and θ is the temperature difference between the actual and initial or reference temperature. The equation, by means of which we can resolve the problem using the axial force, is as follows according to Wear, Timoshenko and Young, *[4]*:

$$EI\frac{\partial^4 w(x,t)}{\partial x^4} + F_T\frac{\partial^2 w(x,t)}{\partial x^2} + \rho A\frac{\partial^2 w(x,t)}{\partial t^2} = 0, \tag{4.6}$$

where E means Young modulus, I area moment of inertia, A area, ρ density of material, t time and w the displacement. Using the method of separation of variables $w(x,t)=X(x)\Omega(t)$ and introducing the new functions, Equation (4.6) can be written down in a slightly less complicated way:

$$c^2\frac{X''''(x)}{X(x)}+2\gamma\frac{X''(x)}{X(x)}-\frac{\ddot{\Omega}(t)}{\Omega}=\omega^2, \tag{4.7}$$

where the partial derivatives have been replaced with total derivatives.

$$\ddot{\Omega}(t)+\omega^2\Omega(t)=0 \tag{4.8}$$

$$X''''(x)+2\gamma X''(x)-\beta^4X(x)=0 \tag{4.9}$$

In Equation (4.7), the new symbols represent the following functional relations:

$$\beta^2=\frac{\omega}{c},c^2=\frac{EI}{\rho A},\ \gamma=\frac{F_T}{2EI} \tag{4.10}$$

Thus, a general solution to Equations (4.8) and (4.9) is ($\lambda=\sqrt{\beta^4+\gamma^2}$):

$$X(x)=C_1\cos\left(\sqrt{\lambda+\gamma}x\right)+C_2\cosh\left(\sqrt{\lambda-\gamma}x\right)+C_3\sin\left(\sqrt{\lambda+\gamma}x\right)+C_4\sinh\left(\sqrt{\lambda-\gamma}x\right) \tag{4.11}$$

$$\Omega(t)=A\sin(\omega t)+B\cos(\omega t) \tag{4.12}$$

In the equation (4.11), the value of λ (where the influence of angular frequency ω is hidden) and three of four constants of integration C_1, C2, C_3, and C_4 are determined from the boundary conditions. The fourth constant is possible to find in the combination with the constants A and B in equation (4.11). For a given beam at a defined temperature, the values by λ depend upon the boundary conditions, *[5-9]*. Using boundary conditions, the following solutions can be analytically computed ($\Gamma=L^2\gamma,\Lambda=L^2\lambda$):

With the known angular frequencies ω_n of individual modes of vibration, it is possible to calculate X_n and Ω_n of individual modes of vibration. To determine the solution for the displacement, we have to solve the equation, *[6-15]*:

$$w(x,t)=\sum_{i=1}^{\infty}\left(A_n\sin(\omega_n t)+B_n\cos(\omega_n t)\right)X_n(x), \tag{4.13}$$

where the modal shapes can be shown to be orthogonal:

$$\int_0^l X_n(x)X_m(x)dx=0\quad for\ n\neq m \tag{4.14}$$

The model presented in our paper is fully analytical, but when compared with the measured results it points to a large deviation from reality, *[6-15]*. The biggest problem with this model is that the clamped wall can fully withstand the beam for the beam to have a constant length all the time in the mathematical model in question. The above assumption is not realistic. As a result, a new model was designed to reduce to at least to some extent the huge differences between the analytical results and the measured values.

4.2 Local Timoshenko beam model under thermal stresses

The Timoshenko beam model, *[6-10]*, includes the effect of rotary inertia and shear deformation. The Timoshenko vibrational beam model gives the next expression:

$$\frac{EI}{\rho A}\frac{\partial^4Y}{\partial x^4}+\frac{F_T}{\rho A}\frac{\partial^4Y}{\partial x^4}+\frac{\partial^2}{\partial t^2}-\frac{l}{A}\left(1+\frac{E}{KG}\right)\frac{\partial^4Y}{\partial x^2\partial t^2}+\frac{I}{A}\frac{\rho}{KG}\frac{\partial^4Y}{\partial t^4} \tag{4.15}$$

$$K=\frac{2(1+\mu)}{4+3\mu} \tag{4.16}$$

In Eq. (4.15), I is the dynamic moment of inertia of the beam, nanotube, K is the shear coefficient of the nanotube, and μ is the Poisson's ratio. F_t presents additional thermal force:

$$F_t=\alpha TEA \tag{4.17}$$

The solution of Eq. (4.15) could be expressed as:

$$Y(x,t)=y(x)e^{-i\omega t} \tag{4.18}$$

In Eq. (4.18), ω is the angular frequency. In the above approximations, the following dimensionless forms can be expressed as:

$$\frac{d^4\eta}{d\zeta^4}+\left[(\alpha+\beta)\Gamma^2+\delta\right]\frac{d^2\eta}{d\zeta^4}-\left(1-\Gamma^{2\alpha}\alpha\beta\right)\Gamma^2\eta \tag{4.19}$$

$$\eta=\frac{y}{L};\zeta=\frac{x}{L},\alpha=\frac{l}{AL^2},\beta=\frac{El}{KGAL^2} \tag{4.20}$$

$$\Gamma=\frac{\rho A\omega^2L^4}{El},\delta=\frac{F_TL^2}{El} \tag{4.21}$$

Where δ represents the effect of thermal vibration of the frequency of SWCNT. The general solution of Eq. (4.19) could be expressed as

$$\eta(\xi)=C_1\cos\left(\sqrt{\lambda-\gamma}\varepsilon\right)+C_2\cosh\left(\sqrt{\lambda+\gamma}\varepsilon\right)+C_3\sin\left(\sqrt{\lambda-\gamma}\varepsilon\right)+C_4\sinh\left(\sqrt{\lambda+\gamma}\varepsilon\right) \tag{4.22}$$

When the solution integrates with the boundary condition for the support-simply support nanotube model we obtain the solution:

$$\Gamma^4-\frac{1+(n\pi)^{2^{(\alpha+\beta)}}}{\alpha\beta}\Gamma^2+\frac{n^2\pi^2}{\alpha\beta}\left(-n^2\pi^2+\delta\right)=0 \tag{4.23}$$

For the case of Euler-Bernouli beam ($\alpha=\beta=0$), we obtain the following equation:

$$\Gamma=n\pi\sqrt{-\delta+(n\pi)^2} \tag{4.24}$$

The presented mathematical model was used to calculate the thermodynamic properties of the state of a pure aluminium microbeam. Table 1 contains the main important data of the beam. The aluminium beam is particularly interesting due to its relatively high expansion coefficients. In the presented section, we have calculated the vibrational characteristics for the supported-simply supported systems. For carbon nanotubes, we have used data for Young modulus and linear expansion coefficient shown in the Prakash Thesis, [16]. Figures 11 and 12 show angular frequency for nanotubes for the first, second and third orders. From both figures, we see that when we have relatively long nanotubes (L/D>10), the results for Timoshenko and Euler-Bernouli model give similar results; in contrast, when we have short nanotubes the Timoshenko model gives much better results for first and higher orders.

Table 1: *Fundamental constants for aluminium beam*

	Beam
Length (m)	$6.35\cdot10^{-2}$
Width (m)	$2.04\cdot10^{-2}$
Thickness (m)	$1.62\cdot10^{-3}$
Young modulus (N/m^2)	$6.9\cdot10^{10}$
Volume expansion coefficient (1/K)	$24\cdot10^{-6}$ K^{-1}
Spring constant (N/m)	$1.553\cdot10^{5}$
Density (kg/m^3)	2780

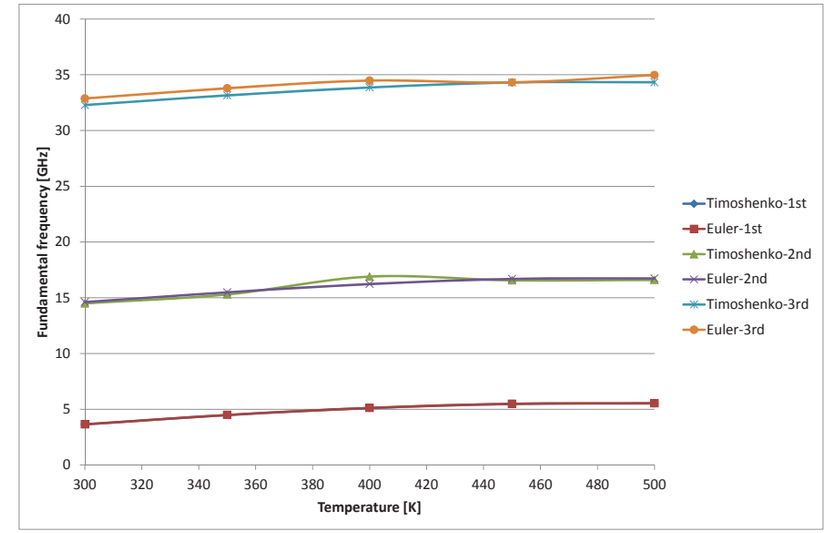

Figure 11: *Fundamental frequency for nanotube with L/D=40 with Timoshenko and Euler-Bernouli model*

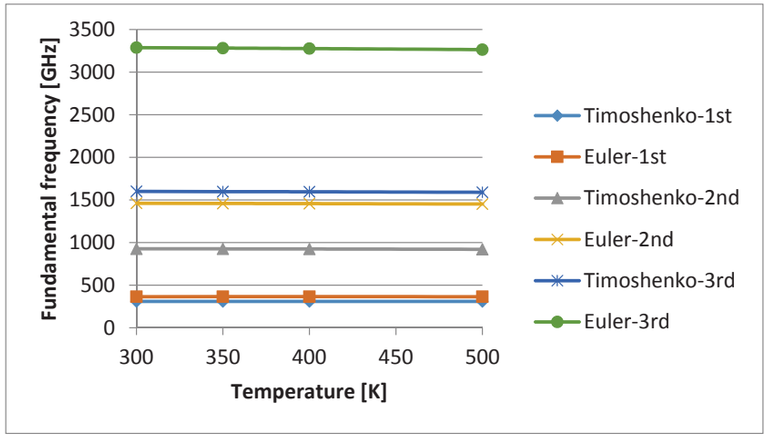

Figure 12: *Fundamental frequency for nanotube with L/D=4 with Timoshenko and Euler-Bernouli model*

References

[1] **N. Savage**: Super carbon, Nature, vol. 483, 2012

[2] **Singhal, V., Garrimela, S., Raman, A.:** *Microscale pumping technologies for microchannel cooling systems,* Appl. Mech. Rev., Vol. 57, No.3, p.p. 191-222, p.p. 30-31

[3] **Avsec, J., Oblak, M.:** *The calculation of thermal conductivity, viscosity and thermodynamic properties for nanofluids on the basis of statistical nanomechanics*, *Int. j. heat mass transfer*. [Print ed.], Vol. 50, Iss. 21/22, p.p. 4331-4341, Oct. 2007

[4] **Naterer, G.F., Adeyinka, O.B.:** *Microfluidic Exergy Loss in a Non-Polarized Thermomagnetic Field*, International Journal of Heat and *Mass transfer*, Vol. 48, p.p. 3945-3956, 2005

[5] **Avsec, J**.: *MHD, FHD and PHD fluid flow in microchannels in dependence of temperature and electromagnetic field,* V: RUBINACCI, G. (ur.). 15th International Symposium on Applied Electromagnetics and Mechanics, 7-9 September 2011, Napoli, Italy. Applied electromagnetics and mechanics : proceedings of the 15th International Symposium on Applied Electromagnetics and Mechanics, Napoli, Italy, 7-9 September 2011

[6] **Avsec, J**.: *The vibrations of microbeams and nanotubes*, J. Vibroeng (Vilnius), Vol. 13, Iss. 4, p.p. 638-645, Dec. 2011

[7] **Pastoeiza-Gallego, M.J. Lugo, L., Legido, J.L., Pineiro, M.M.:** *Thermal conductivity and viscosity measurements of ethylene-glycol based Al_2O_3 nanofluids*, Nanoparticles research Letters, Vol. 221, No.6, p.p.1-11, 2011

[8] **Avsec, J**.: *The combined analysis of phonon and electron heat transfer mechanism on thermal conductivity for nanofluids,* Int. j. heat mass transfer. [Print ed.], Vol. 51, Iss. 19/20, p.p. 4589-4598, Sep. 2008

[9] **Gad-el-Hak, Mohamed:** *The MEMS handbook*, CRC, 2001

[10] **Avsec, J., Praunseis Z., Tršelič I., Novosel, U.**: *The Development of Modern Nano and Micro Energy Technologies*, Enre 2013 conference, Velenje, 2013

[11] **Guz, A., Rushitskii, Ya**.: *Nanomaterials on the Mechanics of Nanomaterials*, International Applied Mechanics, Vol. 39, No. 11, p.p. 1271-1293, 2003

[12] **Marques, R.F., Inman, D.J. Rade, D.J.:** *Assesment of adaptive techniques for the control of structures subject to temperature variations*, 12th ICSV Conference, Lisbon, Portugal, 2005

[13] **Avsec, J.:** *The Influence of Temperature Field on Vibration Characteristics of Beams and Rotating Shafts*, Journal of Vibroengineering. Vol. 11, Iss. 4, p.p. 665-672, 2009

[14] **Hsu, J.-C., Chang, R.-P., Chang W.-J.**: *Resonance frequency of chiral single-walled carbon anotubes using Timoshenko beam theory*, Phys. Let. A, Vol. 372, p.p. 2757.2759, 2008

[15] **Chang, T., Geng, J., Guo, X**.: *Prediction of chirality-, and size dependent elastic properties of single-walled carbon nanotubes via molecular mechanics model*, proc. Roy. Soc.A, Vol. 462, p.p. 2524-2540, 2006

[16] **Prakash N**.: *Determination of coefficient of thermal expansion of single-walled carbon nanotubes using molecular dynamics simulation*, PhD Thesis, Florida state University, 2005

JET Journal of Energy Technology

JET Volume 8 (2015) p.p. 43-55
Issue 4, December 2015
Typology of article 1.01
www.fe.um.si/en/jet.html

ON THE ISOCHRONICITY OF PERIODIC SOLUTIONS AT A CENTRE MANIFOLD

O IZOHRONOSTI PERIODIČNIH REŠITEV NA CENTRALNI MNOGOTEROSTI

Brigita Ferčec[1,2]✉, Matej Mencinger[3,4]

Keywords: centre manifold, centre problem, isochronicity

Abstract

The problem of isochronicity is discussed from the historical and dynamical systems point of view. The model of Huygen's cycloidal chops is mathematically explained. We consider two dynamical systems arising from a three-dimensional system with a centre manifold. Based on the period function approach we find necessary and sufficient criteria on the coefficients of the system to distinguish between the cases of isochronous and non-isochronous oscillations.

Povzetek

Problem izohronosti je obravnavan s stališča dinamičnih sistemov ter iz zgodovinskega stališča. Matematično je razložen Huygensov model ure s cikloidnim nihalom. Na osnovi analize funkcije periode obravnavamo dva dinamična podsistema tridimenzionalnega sistema s centralno mnogoterostjo in poiščemo potrebne in zadostne pogoje za izohronost centra na raznoterosti določeni s koeficienti sistema.

✉ Corresponding author: Matej Mencinger, Tel.: +386 2 229 4321, Mailing address: University of Maribor, Faculty of Civil Engineering, Transportation Engineering and Architecture, Smetanova ulica 17, 2000 Maribor, Slovenia. E-mail address: matej.mencinger@um.si
[1] University of Maribor, Faculty of Energy Technology, Hočevarjev trg 1, 8270 Krško, Slovenia
[2] Center for applied mathematics and theoretical physics, University of Maribor, Mladinska 3, SI-2000 Maribor, Slovenia

[3] University of Maribor, Faculty of Civil Engineering, Transportation Engineering and Architecture, Smetanova ulica 17, 2000 Maribor, Slovenia
[4] Institute of Mathematics, Physics and mechanics, Jadranska 19, 1000, Ljubljana, Slovenia

1 INTRODUCTION

A simple pendulum is a bob of mass m on a massless rigid wire of length l (see Fig. 1). Assuming no damping (i.e. the only force acting on the system is the weight of the bob), the differential equation governing a simple pendulum is

$$\frac{d^2\varphi}{dt^2}+\frac{g}{l}\cdot\sin\varphi=0 \tag{1.1}$$

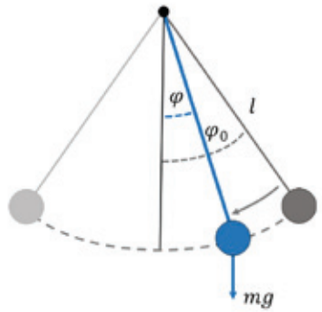

Figure 1: *A simple pendulum of length l driven by the weight $F=-mg$ of the bob.*

There are several approximations for a period of a simple pendulum (see Fig.1) of length l. One of them (see [1]) is

$$T(l;\varphi_0)=2\pi\left(\frac{\varphi_0}{\sin\varphi_0}\right)^{\frac{3}{8}}\cdot\sqrt{\frac{l}{g}}, \tag{1.2}$$

where φ_0 is the initial angle displacement (amplitude) of the bob.

Note that substituting $x=\frac{d\varphi}{dt}$, $y=\varphi$ and $\tau=\sqrt{\frac{g}{l}}\cdot t$ into (1.1) one can easily derive the following system

$$\frac{dx}{d\tau}=-\sin y\approx -y+\frac{y^3}{3!}-\cdots,\quad \frac{dy}{d\tau}=x. \tag{1.3}$$

The qualitative behaviour of this system is determined by how $x(\tau)$ and $y(\tau)$ behave with the change of τ. It is convenient to indicate how a solution behaves in the phase plane, that is in the x,y −plane. The qualitative behavior is represented by a family of curves, directed with increasing τ. These phase curves are called trajectories or orbits of system (1.1.3). The geometrical representation of the qualitative picture of orbits of system (1.1.3) is called its phase portrait. System (1.1.3) admits a centre at $(0,0)$, that is, all the orbits close to the origin are closed or, in other words, the origin is enclosed with simple closed curves (solutions are periodic). Obviously,

because of (1.1.2) the centre of (1.1.3) is not isochronous, i.e. not all periodic solutions have the same period. Isochronicity, as will be stated in the next section (see Definition 2), was not known at the time of the great Dutch astronomer, physicist and mathematician Christian Huygens. However, he was aware that if the amplitude of the pendulum's swing changed, the time of swing would also change, which means that the pendulum was not isochronous, [2]. In the limit of small amplitudes, the period (1.1.2) is approximated by $T(l)=2\pi\cdot\sqrt{\frac{l}{g}}$. The following system is obtained from the equation of a mathematical pendulum (1.1) (again using the change of time $\tau=\sqrt{\frac{g}{l}}\cdot t$)

$$\frac{dx}{d\tau}=-y,\quad \frac{dy}{d\tau}=x. \tag{1.4}$$

However, for larger amplitudes, the period T is a function of the amplitude. The approximation formula (1.1.2) is just one of many existing [1]. Huygens' ingenious idea, which he put into practice, was to vary the effective length of the pendulum by allowing its cord to wrap partially around an obstruction as it swings. What should the shape of this obstruction be in order to ensure that the period is strictly independent of the amplitude?

In the middle of the 17th century, the accuracy of clocks was not measured in minutes; even the best of them gained or lost several minutes per day because they were driven by falling weights or springs. Galileo Galilei was probably the first who wanted to design a pendulum driven clock in order to achieve better accuracy. He believed that he had mathematically proven that a (simple) pendulum is isochronous. As already stated, for the case of the pendulum this simply means that the time it takes to complete one full swing is independent of the size of the swing. Nowadays, it is well-known that this is not the case, and that Galileo was mistaken (see approximation formula (1.1.2)). The first scientist who produced a pendulum-driven clock to keep time errors to within one minute per day was Christian Huygens in 1656; within two years the clocks with accuracy of about 10 seconds per day were produced (by Huygens and others).

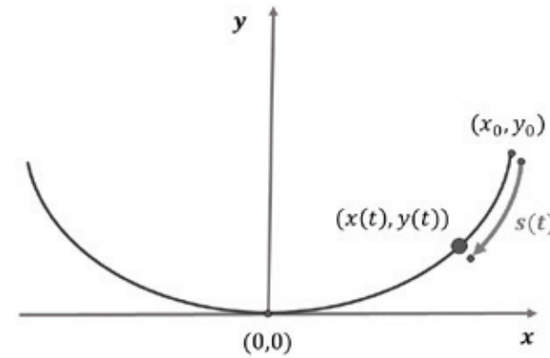

Figure 2: *A bead on a wire of shape* $(x(t),y(t))$.

In order to solve the problem of an "isochronous pendulum", a generalization of the simple pendulum in the sense depicted in Fig. 2 was considered. Thus, if we allow the shape connecting $(\mathbf{x_0}, \mathbf{y_0})$ with $(\mathbf{0}, \mathbf{0})$ to be different from a semicircle (i.e. a general shape $(\mathbf{x(t)}, \mathbf{y(t)})$), then Huygens's question (of isochronous swing) becomes for what shape will the bead descend to the origin in the same time regardless of its starting point $(\mathbf{x_0}, \mathbf{y_0})$?

Denoting by $s(t)$ the distance along the string that the bead has traveled at time t and by $v(t) = \frac{ds}{dt} = \sqrt{\left(\frac{dx}{dt}\right)^2 + \left(\frac{dy}{dt}\right)^2}$ the velocity of the bead (at time t) which is (in contrast) equal to $v(t) = -\sqrt{2g(y_0 - y(t))}$, where g is the acceleration of a freely falling body due to gravity. Furthermore, assume that the functorial dependence of $s(t)$ in terms of $y(t)$ is $s = f(y)$. Then the time taken by a bead to descend from (x_0, y_0) to $\big(x(t), y(t)\big)$ becomes:

$$T(y; y_0) = \int_{y_0}^{0} \frac{dt}{ds}\frac{ds}{dy}dy = \int_{y_0}^{0} \frac{-1}{\sqrt{2g(y_0 - y)}} f'(y)dy. \tag{1.5}$$

Substituting a dimensionless variable $z = \frac{y}{y_0}$ into (1.1.5) and rearranging we obtain

$$T(z) = \frac{1}{\sqrt{2g}} \int_0^1 \frac{f'(zy_0)\sqrt{y_0}}{\sqrt{1-z}} dz, \tag{1.6}$$

which is independent of y_0 (i.e. a constant function of y_0) for $0 < z < 1$, if $f'(zy_0)\sqrt{y_0}$ is a function only of z (and not of y_0). This is equivalent to $\frac{\partial}{\partial y}\left(f'(zy)\sqrt{y}\right) = 0$ or explicitly

$$2f''(u)u + f'(u) = 0; \;\; 0 < u < y_0, \tag{1.7}$$

where $u = zy$.

Obviously, the solution to (1.1.7) expressed in terms of y as independent variable is $f(y) = C_1 + C_2\sqrt{y}$. This implies

$$f'(y) = \sqrt{\frac{C}{y}}, \qquad C > 0. \tag{1.8}$$

Recall that $s = f(y)$, yielding $\frac{ds}{dy} = f'(y)$. Dividing $\left(\frac{ds}{dt}\right)^2 = \left(\frac{dx}{dt}\right)^2 + \left(\frac{dy}{dt}\right)^2$ by $\left(\frac{dy}{dt}\right)^2$ yields $\left(\frac{ds}{dy}\right)^2 = (f'(y))^2 = \left(\frac{dx}{dy}\right)^2 + 1$ and finally from (1.1.8) we obtain

$$x = \int_{y_0}^{y} \sqrt{\frac{C - y}{y}} dy. \tag{1.9}$$

The solution to (1.1.9) containing $(x, y) = (0,0)$ can be parametrized (using $y = C\sin^2\frac{\varphi}{2}$, for $0 < \varphi < \pi$, and the "half angle identities") by

$$x(\varphi) = \frac{C}{2}(\varphi + \sin\varphi), \qquad y(\varphi) = \frac{C}{2}(1 - \cos\varphi), \tag{1.10}$$

which passes through (x_0, y_0) for $\varphi = \varphi_0 \leq \tan^{-1}\frac{2}{\pi}$ (satisfying $\frac{y_0}{x_0} = \frac{1-\cos\varphi_0}{\varphi_0 + \sin\varphi_0}$) and $C = \frac{2y_0}{1-\cos\varphi}$. The shape of the curve $(x(t), y(t))$ from (1.10) is called an (inverted) cycloid (see Fig. 3).

Definition 1. The cycloid (studied and named by Galileo in 1599) is the locus of a point on the rim of a circle of radius *a* rolling along a straight line. If the point considered on a circumference of the rolling circle is initially in the origin (0,0), the cycloid has a cusp at the origin and its humps are oriented upward. Its parametric equation is

$$x(t) = a(t - \sin t), \;\; y(t) = a(1 - \cos t) \tag{1.11}$$

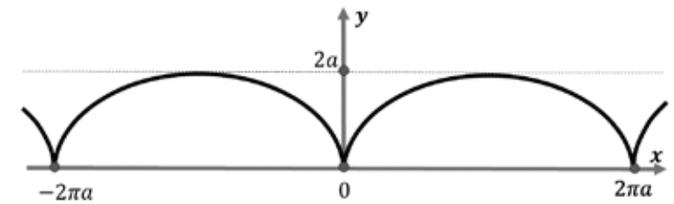

Figure 3: *Cycloid: The path followed by a point on the circumference of a circle as that circle rolls along a straight line.*

An involute is a curve obtained from another given curve by attaching an imaginary taut string to the given curve and tracing its free end as it is (un)wound onto that given curve. *The evolute* of a curve is the locus of all its centres of curvature. That is to say that when the centre of curvature of each point on a curve is drawn, the resultant shape will be the evolute of that curve. For instance: the evolute of a circle is a single point at its centre, the evolute of a quadratic parabola $y = x^2$ is a semicubical parabola $y = \frac{1}{2} + \frac{3}{4}\sqrt[3]{4x^2}$. The only curve for which the evolute (and involute) is "of the same size" (neglecting translation) as the original curve is the cycloid (see Fig. 3 and Fig. 4). The evolute of an involute is the original curve (fewer portions of zero or undefined curvature). Alternatively, another way to construct the involute of a curve is to replace the taut string by a line segment that is tangent to the curve on one end, while the other end traces out the involute (Fig. 3).

Figure 4: *Inverted cycloid (black) with its involute (red) which is a (inverted) cycloid with the same parameter a, just translated for a vector $(\pi a, -2a)$.*

The above results led Huygens to invent a pendulum with cycloidal chops (Fig. 5).

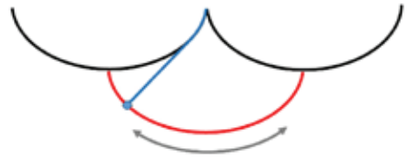

Figure 5: *The cycloidal chops pendulum invented by C. Huygens.*

However, it is not possible to determine the centre of oscillation for pendula suspended between cycloids, as seen in Fig. 4, since the motion of a pendulum with cycloidal chops is not planar (which was known by Huygens; such a pendulum is a multiple system, i.e. a system having two degrees of freedom). Therefore, the next step of improvements of the pendulum clocks was the so-called escapement mechanism (which was driven primarily by the gravity force and later by the force of a spring).

2 ISOCHRONICITY OF PLANAR SYSTEMS OF ORDINARY DIFFERENTIAL EQUATIONS

We discuss differential systems with analytical right sides

$$\frac{dx}{dt} = -y + \sum_{i+j=2}^{\infty} p_{ij} x^i y^j, \frac{dy}{dt} = x + \sum_{i+j=2}^{\infty} q_{ij} x^i y^j, \tag{2.1}$$

where p_{ij} and q_{ij} are real constants. There has been a longstanding problem, [3], called the Poincaré centre-focus problem; for the system (2.1) to find explicit conditions under which (2.1) has a *centre at the origin*. The problem is equivalent to an analogue for a corresponding periodic equation

$$\frac{dr}{d\varphi} = \frac{\sum_{i=1}^{\infty} A_i(\varphi) r^{i+1}}{1 + \sum_{i=1}^{\infty} B_i(\varphi) r^i} = \sum_{i=2}^{\infty} R_i(\varphi) r^i \tag{2.2}$$

to have periodic solutions. To see this let us note that the phase curves of (2.1) near the origin in polar coordinates $x = r\cos\varphi$, $y = r\sin\varphi$ are determined by (2.2), where $A_i(\varphi)$ and $B_i(\varphi)$ are polynomials in $\cos\varphi$ and $\sin\varphi$ and $R_i(\varphi)$ are 2π −periodic functions of φ and the series on the right-hand side of (2.2) is convergent for all φ and all sufficiently small r, [4].

Since the closed orbits of (2.1) correspond to periodic solutions of (2.2), the planar analytic vector field (2.1) has a centre at (0,0) if and only if (2.2) has a centre at $r = 0$; that is, all the solutions nearby are periodic.

All methods for determining the nature of the critical point of (2.1) theoretically require determining infinitely many coefficients of some function or as we will see later the corresponding ideal of the infinitely many polynomials, [4,5,6,7]. The most widely used method to resolve the Poincare centre-focus problem are the so-called Lyapunov method (combined with the Bautin method) and Mironenko's method, [8]. Solving the Poincaré centre-focus problem for a given system (2.1) may be a tedious job. However, once we know the origin of (2.1) is a centre, the problem of isochronicity becomes sensible, and the definition of the period function makes sense.

Definition 2 ([4]). Suppose $r^* > 0$ is so small that it lies in the so-called period annulus (the maximal neighbourhood of the origin that is enclosed with simple closed curves). Let us consider the line segment $\sum = \{(x, y): 0 < x < r^*, y = 0\}$. For any $x = (r, 0) \in \Sigma$ satisfying $0 < r < r^*$ let $T(r)$ denote the least period of the corresponding trajectory (through $(x, y) = (r, 0) \in \Sigma$). The function $T(r)$ is the *period function* of the centre. If the function $T(r)$ is constant, then the centre $(0,0)$ of (2.1) is said to be *isochronous.*

In (2.2), the corresponding time-dependent equations are of the form

$$\frac{dr}{dt} = \sum_{i=1}^{\infty} A_i(\varphi) r^{i+1} \tag{2.3}$$

and

$$\frac{d\varphi}{dt} = 1 + \sum_{i=1}^{\infty} B_i(\varphi) r^i. \tag{2.4}$$

For a sufficiently small (fixed) r_0 a solution to (2.3) satisfying the initial condition $(r, \varphi) = (r_0, 0)$ has a unique solution $r(\varphi) = f(\varphi; r_0)$. Inserting $f(\varphi; r_0)$ into (2.4) yields

$$\frac{dt}{d\varphi} = \frac{1}{1+\sum_{i=1}^{\infty} M_i(\varphi) r_0^i} = 1 + \sum_{i=1}^{\infty} F_i(\varphi) r_0^i.$$

After integration, we obtain

$$t - \varphi = \sum_{i=1}^{\infty} \Theta_i(\varphi) r_0^i, \tag{2.5}$$

where $\Theta_i(\varphi) = \int_0^{\varphi} F_i(\varphi)d\varphi$ and the series on the right-hand side of (2.5) is convergent (for small enough $0 < r_0 < r^*$) and $0 \le \varphi \le 2\pi$. For any $(r_0, 0) \in \Sigma$ for $\varphi = 2\pi$ we write $t = T$ and obtain

$$T(r_0) = 2\pi\left(1 + \sum_{i=1}^{\infty} T_i r_0^i\right), \tag{2.6}$$

where $T_i = \frac{\Theta_i(2\pi)}{2\pi}$. No, we can finally state the condition for isochronicity of the centre.

Suppose system (2.1) has a centre at the origin, then $(0,0)$ is isochronous if and only if $T_i = 0$ for all $i \in \mathbb{N}$. Thus, the set of all systems (2.1) with isochronous centre on the centre manifold is the set of common zeros of polynomials $T_i(p_{ij}, q_{ij})$. Thus, we have to consider the ideal $I = \langle T_1(p_{ij}, q_{ij}), T_2(p_{ij}, q_{ij}), T_3(p_{ij}, q_{ij}), \dots \rangle$. According to the Hilbert Basis Theorem (see [9]), every ideal in the polynomial ring over a field is finitely generated, and then the direct consequence of this theorem is that the ascending chain of ideals $I_1 = \langle T_1(p_{ij}, q_{ij}) \rangle$, $I_2 = \langle T_1(p_{ij}, q_{ij}), T_2(p_{ij}, q_{ij}), \dots \rangle$, stabilizes. That is, there exists $m \ge 1$ such that ideal I with infinitely many polynomials $T_i(p_{ij}, q_{ij})$ is the same as I_m.

3 CENTRE MANIFOLDS

The theory of centre manifolds, which originates from the works of V. A. Pliss, [10,11], and was then further developed by many others (see, e.g. [12,13] and references therein) is an extremely effective tool for studying the behaviour of trajectories of high-dimensional systems of ordinary differential equations. Note that one of the important applications of centre manifolds (also called the Pliss reduction principle, [11]) is that it allows the reduction of the system and consequently the study of the stability in lower dimensional phase space (thus, instead of analysing the original high-dimensional phase space we can consider the lower-dimensional subsystem).

Consider an $\mathbf{m} + \mathbf{n}$-dimensional system of ordinary differential equations of the form

$$\begin{aligned} \dot{x} &= Ax + u(x, y) \\ \dot{y} &= By + v(x, y), \end{aligned} \tag{3.1}$$

where $x \in \mathbb{R}^m, y \in \mathbb{R}^n$, $\mathrm{Re}(\sigma(A)) = 0$, $\mathrm{Re}(\sigma(B)) \neq 0$, $\sigma(A)$ and $\sigma(A)$ are spectrums of A and B, respectively, and u, v are C^k- functions, $k \ge 1$ which vanish together with their first derivatives

at the origin. By definitio, a C^k- manifold $W^c \equiv W\hat{}c(0, U)$ in a neighbourhood U of 0 is said to be a centre manifold of (3.1) if W^c is invariant under the flow as long as the solution remains in U nd W^c is the graph of a C^k- function $y = h(x)$ which is tangent at $(0,0) \in \mathbb{R}^m \times \mathbb{R}^n$ to the x-space.

The following fundamental result shows that for the system (3.1), there is always a centre manifold in a neighbourhood of the origin.

Theorem 1 ([12]). There exists a neighbourhood U of $(0,0) \in \mathbb{R}^m \times \mathbb{R}^n$ such that there exists a local centre manifold W^c of (3.1) which is the graph of *a* C^k- function $y = h(x)$.

The simplest examples of the centre manifolds can be seen in low dimensions. For instance, consider two-dimensional system

$$\dot{x} = -x^3, \quad \dot{y} = -y. \tag{3.2}$$

For any constants c_1, c_2 the curve $h(x; c_1, c_2)$, where

$$y = h(x; , c_1, c_2) = \begin{cases} -c_1 e^{-\frac{1}{2x^2}}, & x < 0 \\ 0, & x = 0 \\ c_2 e^{-\frac{1}{2x^2}}, & x > 0, \end{cases}$$

consists of orbits of (3.2) and is therefore invariant. Furthermore, this curve is tangent to the x-axis at the origin, which implies that it is a centre manifold. From this example, we can also see that the centre manifold is not necessaily unique. Another simple two-dimensional system with a centre manifold is

$$\dot{x} = -x^3, \quad \dot{y} = -y + x^2.$$

Similar as in the previous case, we see that although the system is analytic, it is not difficult to verify that the centre manifold is not analytic.

In three dimension, a family of systems with a centre manifold is

$$\begin{aligned} \dot{u} &= -v + P(u, v, w) \\ \dot{v} &= u + Q(u, v, w) \\ w &= -\lambda w + R(u, v, w), \end{aligned} \tag{3.3}$$

where λ is a positive real number and P, Q, R are polynomials without constant and linear terms. By Theorem 1, this system has a centre manifold $w = f(u, v)$. There are many systems arising from physics (for instance, the Rikitake system [14], for Earth's magnetic field or the Hide-Acheson Dynamo, [15]) that possess a fixed point at which the linear part has one negative and two purely imaginary eigenvalues and are therefore of the form (3.3). Since system (3.3) has a centre manifold W^c and $\lambda > 0$, the trajectories in a small neighbourhood of the origin tend to the trajectories to the centre manifold as time increases. In systems (3.3), the phase portrait in a neighbourhood of the origin on W^c can be, depending on the added nonlinear terms P and Q, either a centre in which case every trajectory (other than the origin itself) is an oval surrounding the origin, or a focus, in which case every trajectory spirals towards the origin or every trajectory spirals away from the origin as the time increases. The problem of determining the dynamical

behaviour on W^c, that is, distinguishing between a centre and a focus on the centre manifold for a quadratic polynomial system of the form (3.3) was studied in [16].

4 THE STUDY OF TWO EXAMPLES

In [16], the authors studied the dynamics of trajectories at the centre manifolds for the system

$$\begin{aligned} \dot{u} &= -v + au^2 + av^2 + cuw + dvw \\ \dot{v} &= u + bu^2 + bv^2 + euw + fvw \\ \dot{w} &= -w + Su^2 + Sv^2 + Tuw + Uvw, \end{aligned} \tag{4.1}$$

where the coefficients $a, b, c, d, e, f, S, T, U$ are real. They found five conditions for the existence of a centre on the centre manifold:

1. $S = 0$;
2. $a = b = c + f = 8c + T^2 - U^2 = 4(e - d) - T^2U^2 = 2(e + d) + TU$ and $S = 1$;
3. $a = b = c = f = d + e = 0$ and $S = 1$;
4. $d + e = c = f = T - 2a = U - 2b = 0$ and $S = 1$;
5. $c = d = e = f = 0$ and $S = 1$.

The next question that naturally arises is whether the centre at the centre manifold is isochronous, that is, whether all oscillations have the same period. In this paper we study two subfamilies of system (4.1) satisfying conditions 1 and 2 above. For each system, we compute the period function as described in section 2 and use it to find conditions for the centre to be isochronous.

System (4.1) satisfying condition 1 above is written as

$$\begin{aligned} \dot{u} &= -v + au^2 + av^2 + cuw + dvw \\ \dot{v} &= u + bu^2 + bv^2 + euw + fvw \\ \dot{w} &= -w + Tuw + Uvw. \end{aligned} \tag{4.2}$$

It is proven (see [16]) that $w = 0$ isthe centre manifold for system (4.2). The corresponding 2D system

$$\begin{aligned} \dot{u} &= -v + au^2 + av^2 \\ \dot{v} &= u + bu^2 + bv^2 \end{aligned} \tag{4.3}$$

has a centre at the origin for all $a, b \in \mathbb{R}$ (see [16]).

We now study the isochronicity problem for the above centre. Using the computer algebra software MATHEMATIC, we first turn to the computation of the period function T of the form (2.6). After introducing polar coordinates system, (4.3) becomes

$$\begin{aligned} \frac{dr}{dt} &= r^2(a\cos\varphi + b\sin\varphi) \\ \frac{d\varphi}{dt} &= 1 + r(b\cos\varphi - a\sin\varphi). \end{aligned} \tag{4.4}$$

Following the procedure described in the second section, we find that the first non-zero coefficient of the period function is $T_2 = 2\pi(a^2 + b^2)$. Thus we see that the necessary condition for the isochronicity of system (4.3) is $a = b = 0$, which, obviously is also the sufficient condition.

In the case of conditions 2, under the same renaming of parameters c, d, e, f, T, U and using α, β as in [16], the system (4.1) takes the form

$$\begin{aligned} \dot{u} &= -v - \frac{1}{2}\alpha\beta uw - \frac{1}{2}\beta^2 vw \\ \dot{v} &= u + \frac{1}{2}\alpha^2 uw + \frac{1}{2}\alpha\beta vw \\ \dot{w} &= -w + u^2 + v^2 + (\alpha + \beta)uw + (\beta - \alpha)vw. \end{aligned} \tag{4.5}$$

A search for invariant algebraic surfaces led to the explicit equation of centre manifold W^c given by $w = \frac{u^2+v^2}{1-\alpha u-\beta v}$. Inserting the expression for w into system (4.5), we obtain the system

$$\begin{aligned} u &= -v - \frac{\beta(\alpha u + \beta v)(u^2 + v^2)}{2(1 - \alpha u - \beta v)} \\ v &= u + \frac{\alpha(\alpha u + \beta v)(u^2 + v^2)}{2(1 - \alpha u - \beta v)}. \end{aligned}$$

Using Taylor series expansion up to the order five, we obtain the system

$$\begin{aligned} \dot{u} &= -v + \frac{1}{2}\beta(\alpha u + \beta v)(u^2 + v^2) + \frac{1}{2}\beta(\alpha u + \beta v)^2(u^2 + v^2) + m_1 \\ v &= u - \frac{1}{2}\alpha(\alpha u + \beta v)(u^2 + v^2) - \frac{1}{2}\alpha(\alpha u + \beta v)^2(u^2 + v^2) + m_2, \end{aligned} \tag{4.6}$$

where

$$\begin{aligned} m_1 = \frac{1}{120}(&-60\alpha^3\beta u^5 - 180\alpha^2\beta^2 u^4 v + 10u^3v^2(-6\alpha^3\beta - 18\alpha\beta^3) \\ &+10u^2v^3(-18\alpha^2\beta^2 - 6\beta^4) - 180\alpha\beta^3 uv^4 - 60\beta^4 v^5) \end{aligned}$$

and

$$\begin{aligned} m_2 = \frac{1}{120}(&60\alpha^4 u^5 + 180\alpha^3\beta u^4 v + 10u^3v^2(6\alpha^4 + 18\alpha^2\beta^2) \\ &+10u^2v^3(18\alpha^3\beta + 6\alpha\beta^3) + 180\alpha^2\beta^2 uv^4 + 60\alpha\beta^3 v^5). \end{aligned}$$

Further computation following the computational pattern described in section 2 yields $T_2 = \frac{\pi}{2}(\alpha^2 + \beta^2)$, yielding the following result.

System (4.6) has an isochronous centre if and only if $\alpha = \beta = 0$.

5 CONCLUSIONS

After more than 300 years, the isochronicity problem remains one of the central problems in the theory of dynamical systems. In addition to the period function approach, there are some other approaches. The analysis of the isochronicity problem leads us first to conditions for existence of periodic solutions, i.e. the existence of centre and then the further study yields the conditions on parameters of considered system for the cases of isochronous and non-isochronous oscillations. The approach described in Section 2 requires an integration of trigonometric functions and might be too complex for some systems. Therefore, in some cases, we need to find other ways to solve the isochronicity problem. It turns out that the isochronicity problem for system (2.1) is equivalent to the linearizability problem in which we look for an analytic change of coordinates that reduces (2.1) to the canonical linear centre $\dot{x} = -y, \dot{y} = x$ (see e.g. [4] for more details). The theory of the linearizability of planar systems of ordinary differential equations was applied [17] to system (4.1) corresponding to condition 4 above. In fact, for each of the five conditions above we can find the conditions under which the corresponding system can be reduced to canonical linear centre, and we see that they are the same as conditions obtained using the period function approach.

References

[1] **G.E. Hite**: *Approximations for the Period of a Simple Pendulum,* The Physics Teacher, Vol. 43, p.p. 290, 2005

[2] **C. Huygens** *The pendulum clock or geometrical demonstrations concerning the motion of pendula as applied to clocks.* Translated from the Latin and with a preface and notes by Richard J. Blackwell. With an introduction by H. J. M. Bos. Iowa State University Press, Ames, IA, 1986

[3] **H. Poincaré**: *Mémoire sur les courbes définies par une équation différentielle*, J. Math. Pures et. Appl. (Sér. 3), Vol. 7, p.p. 375–422, 1881; (Sér. 3), Vol. 8, p.p. 251–296, 1882; (Sér. 4), Voil. 1, p.p. 167–244, 1885; (Sér. 4), Vol. 2, p.p. 151–217, 1886

[4] **V.G. Romanovski, D.S. Shafer**: *The Center and cyclicity Problems: A computational Algebra Approach,* Boston: Birkhäuser, 2009

[5] **B. Ferčec, X. Chen, V. Romanovski**: *Integrability conditions for complex systems with homogeneous quintic nonlinearities*, Journal of applied analysis and computation, Vol. 1, Iss. 1, p.p. 9 – 20, 2011

[6] **B. Ferčec, J. Giné, Y. Liu, V. Romanovski**: *Integrability conditions for Lotka-Volterra planar complex quartic systems having homogeneous nonlinearities*, Acta applicandae mathematicae, Vol. 124, Iss. 1, p.p. 107 – 122, 2013

[7] **B. Ferčec, J. Giné, M. Mencinger, R. Oliveira**: *The center problem for a 1 : -4 resonant quadratic system,* Journal of mathematical analysis and applications, Vol. 420, Iss. 2, p.p. 1568 – 1591, 2014

[8] **Z. Zhou**: *A New Method for Research on the Center-Focus Problem of Differential Systems,* Abstract and Applied Analysis, Art. ID 926538, 5 p.p., 2014

[9] **D. Cox, J. Little, D. O'Shea**: *Ideals, Varieties, and Algorithms: An Introduction to Computational Algebraic Geometry and Commutative Algebra,* New York: Springer, 3rd edition, 2007

[10] **S.Yu. Pilyugian, G.R. Sell:** *A Biographical Sketch of Victor A. Pliss***,** Journal of Dynamics and Differential Equations, Vol.15, 2003

[11] **V.A. Pliss**: *A reduction principle in the theory of stability of motion*, Izv. Akad. Nauk SSSR Ser. Mat., Vol. 28, p.p. 1297–1324, 1964

[12] **S. Chow, J. K. Hale**: *Methods of Bifurcation Theory*, Springer-Verlag, New York, 1982

[13] **J. Sijbrand:** *Properties of center manifolds,* Trans.~Amer.~Soc., Vol. 289, 431-469, 1985

[14] **R. Rikitake**: *Oscillations of a system of disc dynamos,* Proc. Cambridge Philos. Soc., Vol. 54, p.p. 89-105, 1958

[15] **R. Hide, A. C. Skeldon, D.J. Acheson:** *A study of two novel self-exciting single-disk homopolar dynamos: theory*, Proc. R. Soc. Lond. A , Vol. 452, p.p. 1369-1395, 1996

[16] **V.F. Edneral, A. Mahdi, V.G. Romanovski, D.S. Shafer***: The center problem on a center manifold in* $\mathbb{R}^3$, Nonlinear Anal., Vol. 75, p.p. 2614-2622, 2012

[17] **V. Romanovski, M. Mencinger, B. Ferčec***: Investigation of center manifolds of three-dimensional systems using computer algebra*, Programming and computer software, Vol. 39, iss. 2, p.p. 67-73, 2013

JET Journal of Energy Technology

JET Volume 8 (2015) p.p. 57-68
Issue 4, December 2015
Typology of article 1.04
www.fe.um.si/en/jet.html

DESIGN OF THE VENTILATION AND AIR-CONDITIONING SYSTEM IN AN OFFICE BUILDING

NAČRTOVANJE SISTEMA PREZRAČEVANJA IN KLIMATIZACIJE V POSLOVNI STAVBI

Franc Rihl[R]

Keywords: ventilation and air-conditioning, cooling, heating, ventilation ducts, Brestanica Thermal Power Plant (TEB).

Abstract

This article presents an office building within the Brestanica Thermal Power Plant for which a design of the ventilation and air-conditioning system has been made. First, a brief description of the existing heating and cooling system from the aspect of the operation and the investment contribution is made. Then a ventilation and air-conditioning system is designed based on the geometric characteristics and thermal needs of the building. Calculation of heat losses, selection of an appropriate ventilation and air-conditioning unit, and design of a ventilation duct system are included in the design. The entire system is evaluated from the aspect of investment value.

Povzetek

V članku je predstavljena poslovna stavba v Termoelektrarni Brestanica, za katero se je naredila študija prezračevanja in klimatizacije. Najprej je na kratko opisan obstoječi sistem ogrevanja in hlajenja iz vidika samega delovanja in investicijskega vložka. V nadaljevanju je načrtovan sistem prezračevanja in klimatizacije glede na geometrijske karakteristike in toplotne potrebe.

[R] Corresponding author: Franc Rihl, Faculty of Energy Technology, Tel.: +386 40 792 479, Mailing address: Hočevarjev trg 1, 8270 Krško, E-mail address: franc.rihl1@um.si

V načrtovanje je vključen preračun toplotnih potreb stavbe, izbira ustrezne prezračevalne in klimatske naprave in načrtovanje sistema prezračevalnih kanalov za transport klimatiziranega zraka. Celotni sistem je ovrednoten tudi iz vidika investicijske vrednosti.

1 INTRODUCTION

The aim of this article is to examine the system for heating, cooling, and ventilation in an office building within TEB. The entire study is based on data obtained from TEB; the current embedded system for heating, cooling and ventilation is described based on this data. Furthermore, the total investment costs of both embedded systems are researched and presented.

Based on the size of the business buildings and the calculation of the heat demand, the selection of an appropriate ventilation and air-conditioning unit and the design of the ventilation duct system is presented. This article concludes with an assessment of the investment costs of installing such a system.

2 DESCRIPTION OF THE OFFICE BUILDING

The office building comprises two separate buildings connected by a corridor on the first floor. Therefore, the smaller part of the office building is named 'Part A', where the reception and offices are, and the bigger one 'Part B', where workshops and a warehouse are. The office building is shown in Figure 1.

Figure 1: *The office building*

The office building is physically separated from the production part of TEB. All relevant information about the office building for further calculation were provided by the head of the TEB, and they are shown in Table 1.

Table 1: *The geometrical characteristics of an office building*

	PART A	PART B
Area of the thermal envelope [m²]	2234.22	3980.50
Conditioned volume [m³]	1741.38	6449.47
Net heated volume [m³]	1286.02	5281.44
Usable area [m²]	494.35	1578.40
Length of the zone [m]	28.42	64.90
Width of the zone [m]	11.50	26.05
Height of the floor [m]	2.40	3.16
Number of floors	2	2
Number of rooms	28	60

Climate characteristics depending on the location of the office building are a temperature deficit of 3100 Kday, a projected temperature of -13 °C and an average humidity of 78%. Depending on the projected temperature, this is the 3rd climate area in Slovenia, [1]. These data are used in the calculation of the transmission heat losses.

3 THE EXISTING SYSTEM FOR HEATING, COOLING AND VENTILATION

The office building does not have a common system for heating and cooling, but it has two entirely separate systems that are independently operating. The old system for heating was upgraded before the heating season in 2006. The old oil boiler system was replaced with a gas-condensing boiler system, with a total heat capacity of 400 kW. The system consists of four Buderus Logamax Plus GB162 boilers connected into a cascade and regulated with two Buderus Logamatic 4000 controllers.

Consumption of natural gas is recorded by a remote system, which is directly connected to the connected gas pipeline. Monthly natural gas consumption between 2011 and 2013 is shown in Figure 1. Annual average natural gas consumption for heating of the office building is 25,732.5 Sm³.

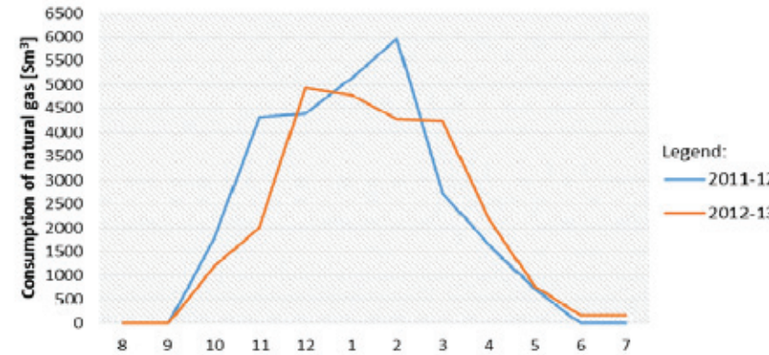

Figure 2: *Consumption of natural gas between 2011 and 2013*

In addition to gas boilers for DHW heating, an air-water heat pump is used. The maximum heat capacity of the heat pump is 5 kW and COP around 2.8. In the event of failure, the old oil boiler system takes over heating, which is connected through a parallel connection and heat exchanger. The total value of the investment in the gas-condensing boiler system was €121,014.86.

The cooling system was mounted in summer 2004. Based on the number of required rooms and necessary cooling capacity, a multi-split unit system was selected. This system consists of 25 units and it is vacuumised and filled with ecologically acceptable R407C liquid. In the entire system is approximately 43 kilos of this cooling fluid. The total value of the investment in the cooling system was €8,863.26.

The office building does not have its own system for ventilation; thus, employees have to provide sufficient air exchange by opening windows and doors. Consequently, this leads to uncontrolled ventilation and heat losses.

4 VENTILATION AND AIR-CONDITIONING SYSTEM

The ventilation and air-conditioning system is concerned with achieving and maintaining thermal comfort parameters in confined areas, [2].

It is a complete process, which includes the production, transport and the injection of the transmission medium into the air-conditioned area. Constant thermal comfort is maintained by regulating the temperature, relative humidity, air velocity, air quality, volume level and differential pressure in the area, [2].

Depending on the scope of operation, two main types of ventilation and air-conditioning system are knowns:

- Comfort, and
- industrial systems, [2].

4.1 Central system for ventilation and air-conditioning

This is the most basic type of a ventilation and air conditioning system from the technical point of view. The transmission medium in this type of system is air. It is accordingly prepared in the central unit; then it is supplied through ventilation ducts in all air-conditioned areas. At the same time, the exhaust air is transported out of the area through the return line of ventilation ducts. Fresh air can be mixed with exhaust air in the mixing chamber in order to reduce energy consumption. However, this mixing process should not significantly affect the thermal comfort in the air-conditioned areas, [2]. An example of the central system for ventilation and the air-conditioning structure is shown in Figure 2.

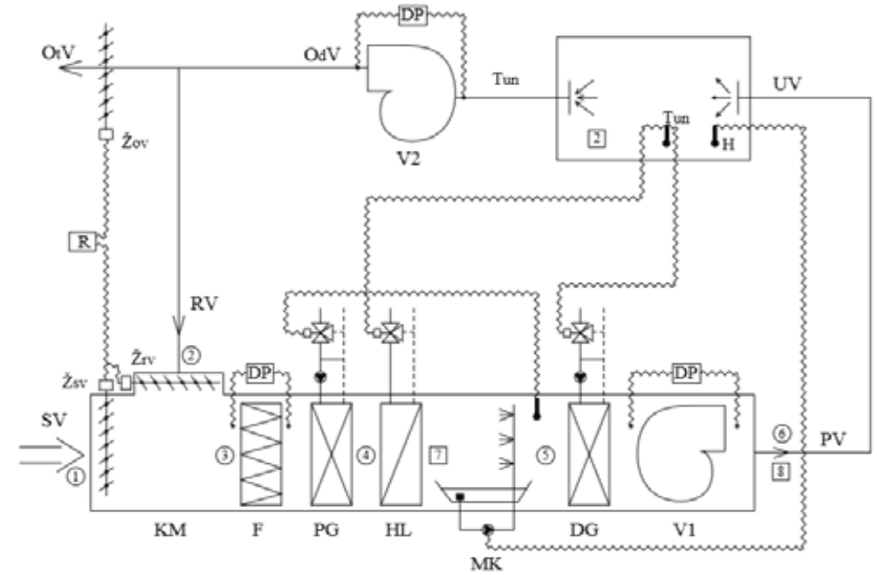

Figure 3: *Structure of the central system for ventilation and air-conditioning*, [2]

5 DESIGN OF VENTILATION AND AIR-CONDITIONING SYSTEM

The design of a ventilation and air-conditioning system includes a calculation of the heating and cooling load of the building according to the information in Table 1. Then, based on the calculated loads and climate data, the size of the central ventilation and air-conditioning unit is chosen. This is done with a numeric program that determines the size of the heater, cooler, heat recovery system and other parts of the system.

After the central ventilation and air-conditioning unit is chosen, a ventilation duct system for transporting air into air-conditioned areas must be designed. This is made by a calculation of ducts dimensions on the basis of the arrangement of the rooms and required air exchange rate. In ventilation ducts, pressure drops occur. Ducts must be designed in such a manner that the fan in the central ventilation and the air-conditioning unit can cover the maximum calculated pressure drop in the system.

5.1 Thermal and cooling load

The thermal load is calculated on the basis of the transmission heat losses of the building and data on the climate in which the building is placed. Cooling load is calculated as the sum of the transmission heat losses and heat gains specified in the German standard VDI 2076. The heat gains described in VDI 2076 are those due to the presence of people, solar radiation gains, the heat of equipment and lighting. Transmission heat losses were calculated in the program URSA GF 4.0, which is made for calculating the thermal protection of buildings and energy use in

buildings in accordance with the regulation on energy efficiency PURES 2010. The data in Table 2 are calculated using Equations 5.1 to 5.4 and the program URSA GF 4.0.

$$\dot{Q}_{HL} = \dot{Q}_T \cdot \Delta T \tag{5.1}$$

$$\dot{Q}_p = \left(\dot{Q}_{p_{tr}} + \dot{Q}_{p_r}\right) \cdot N \tag{5.2}$$

$$\dot{Q}_M = 4 \cdot A_u \tag{5.3}$$

$$\dot{Q}_S = \left[A_i \cdot I_{max} + \left(A - A_i\right) \cdot I_{difmax}\right] \cdot b \cdot s_a \tag{5.4}$$

Table 2: *Calculated data for thermal and cooling load*

	PART A	PART B
Thermal load		
Transmission heat losses [W]	36,145.23	63,931.23
Cooling load		
Transmission heat losses [W]	6,571.86	11,624.46
Heat gains due to people presence [W]	4,945.00	9,890.00
Heat of the devices and lighting [W]	1,977.40	6,313.60
Solar radiation gains [W]	26,800.66	26,907.45
Total cooling load [W]	40,294.92	54,735.51

5.2 Selection of the ventilation and air-conditioning unit

The company Menerga Ltd. has helped with the selection of a ventilation and air-conditioning unit. This company is primarily engaged in ventilation and air-conditioning systems. According to the data calculated in Table 2, they have selected an Adconair 76 ventilation and air-conditioning unit with the counterflow plate heat exchanger and an air compressor cooling system. For Part A, an Adconair Ad 761601 IMH unit was selected with a heat capacity of 55.99 kW, a cooling capacity of 41.87 kW and a 92% heat recovery rate. For Part B, an Adconair Ad 761501 IMH unit was selected with a heat capacity of 87.53 kW, a cooling capacity of 55.45 kW and a 93% heat recovery rate.

Despite all the characteristics, units do not have an integrated system for heating the water heaters. A solution to this manner had to be found, which was the design of the pipeline from the gas condensing boilers to both units.

5.2.1 Design of the pipeline

The pipeline has to connect gas condensing boilers and both units and provide the required heat capacity. The transmission medium in the pipeline is water, and the operating temperature is 70/50 °C. The pipeline consists of several main elements:

- pipes,
- heat exchanger,
- expansion vessel, and
- water pump.

Due to the required heat capacity of the water heaters, the pressure drop in the pipeline, and the velocity of medium and thermal insulation of pipes, a Danfoss XB 59M-1 70 heat exchanger, an OPTIMA 200 expansion vessel, Uponor Ecoflex Thermo Twin 2×63×5.8/200 DN50 pipes and a Grundfos Magna3 50-40 water pump have been selected.

5.3 The dimensions of ventilation ducts

In the office building, a dual ventilation duct system was designed for each part of the building. This was done on the basis of the technical characteristics of the ventilation and air-conditioning units.

The first step was the selection of air velocity through different elements of the ventilation duct system. Recommended values of air velocity are shown in Table 3.

Table 3: *Recommended values of air velocity through different elements of the ventilation duct system*, [3]

Element	The approximate values of the air speed [m/s]	
	Comfort system	Industrial system
Protective gratings	2–4	4–6
Main ducts	4–8	8–12
Side ducts	3–5	5–8
Air diffusers	1,5–2,0	3–4

The second step is the calculation of the cross-section of the ventilation duct according to Equation 5.5 [3].

$$A_{PK} = \frac{\dot{V}}{3600 \cdot w} \tag{5.5}$$

When the calculation of cross-sections of all ducts is done, it is necessary to select a sufficiently large ventilation duct. Recommended sizes of the rectangular ventilation ducts are shown in Table 4.

Table 4: *Recommended sizes of the ventilation ducts,* [3]

Designation	b	h	Surface [m²]
300/150	300	150	0.0450
400/200	400	200	0.0800
500/250	500	250	0.1250
600/300	600	300	0.1800
600/350	600	350	0.2100
700/400	700	400	0.2800
800/500	800	500	0.4000
1000/500	1000	500	0.5000

Protective gratings are selected using Equation 5.6, for which the required effective surface must be larger than the calculated [4].

$$A_{ef2} = B1 \cdot \left(H1 - 21 - \left(7 \cdot n\right)\right) \tag{5.6}$$

The air diffusers are selected according to the required effective surface and injecting speed of air via diagrams, which can be found for special types of diffuser, [4].

5.4 The calculation of the pressure drop in the ventilation ducts

For the ventilation duct system, it is necessary to calculate the maximum possible pressure drop and verify whether it can be covered with the air fans built in the ventilation and air-conditioning units. The maximum possible pressure drop typically occurs in the longest duct. The pressure drop is caused by two types of pressure drops:

- linear, and
- local.

Typically, these pressure drops are calculated using Equations 5.7 to 5.10.

$$\Delta p = \sum \Delta p_{lin} + \sum \Delta p_{lok} \tag{5.7}$$

$$\Delta p_{lin} = \frac{\varepsilon \cdot \rho \cdot w^2}{d_H \cdot 2} \cdot L \tag{5.8}$$

$$d_H = \frac{2 \cdot a \cdot b}{a + b} \tag{5.9}$$

$$\Delta p_{lok} = \zeta \cdot \frac{\rho \cdot w^2}{2} \tag{5.10}$$

The rooms in which the maximum pressure drops in the system were calculated are shown in Table 5.

Table 5: *Calculated pressure drops in the ventilation ducts*

Place	Pressure drop	
	Supply [Pa]	Outlet [Pa]
Part A		
Office 1.1	477.78	400.90
Reception	398.64	307.90
Part B		
Office 1325	661.13	583.24
Warehouse	633.54	567.78

All calculated pressure drops are smaller than the maximum allowed pressure drops of the air fans inside the ventilation and air-conditioning units, which means that the system of ventilation ducts is appropriately designed.

6 FINAL VALUE OF THE INVESTMENT

The investment in the ventilation and air-conditioning system consists of several sets. The main sets are the ventilation and air-conditioning units and elements related to their operation, followed by the ventilation duct system, protective gratings, diffusers and works related to the installation of equipment.

The values shown in Table 6 are based on data obtained from different manufacturers, such as Menerga Ltd., NKM Ltd., Hidria Ltd., Danfoss Ltd., Uponor Corporation, Štern Ltd. and Grundfos Ltd.

Table 6: *Total value of the investment*

Type of costs	Total value without VAT [€]
Equipment – ventilation and air-conditioning units	186,147.00
Equipment – pipeline	7,223.39
Installation and mounting costs, additional work	19,500.00
Total value without VAT [€]	212,870.39
VAT 22 % [€]	46,831.49
The final value of the investment [€]	259,701.88

Certain values are assumed, since it is difficult to estimate the exact value of the services. In that manner, the final value of an investment may be different than it would have been if the project is actually performed.

7 CONCLUSION

This paper describes the current situation in terms of thermal comfort in an office building. A major shortcoming is uncontrolled ventilation, an oversized gas condensing system, and insufficient cooling of the entire building. The consequences of such situation are higher maintenance costs, and deficits or surpluses of fresh air, which leads to uncontrolled heat losses

and higher operating costs. In the ventilation and air-conditioning system, such problems do not occur, because the automation maintains optimal thermal comfort.

From the aspect of investment, it can easily be seen that the investment in the designed system is almost twice as high as in the old one. Another disadvantage is the usage of the gas condensing system for heating the water heaters of the designed system. This application has reduced the investment costs. It can be concluded that the designed system would not be worth the investment, because such systems are typically installed in new buildings.

References

[1] *Podatki za pravilnik o učinkoviti rabi energije*, Državna meteorološka služba – METEO [world wide web], available at: http://meteo.arso.gov.si/met/sl/climate/tables/pravilnik-ucinkoviti-rabi-energije/(3. 9. 2015)

[2] **B. Todorović,** *Klimatizacija*, Savez mašinskih i elektrotehničkih inženjera i tehničara Srbije (SMEITS), Beograd, 2005

[3] **Recknagl, Šprenger, Šramek, Češerković,** *Grejanje i klimatizacija*, sedmo, izmenjeno i dopunjeno izdanje, Interklima, Vrnjačka Nanja, 2011

[4] *Distribution and control air,* brochure, Hidria Ltd. [world wide web], available at: http://si.hidria.com/si/klima/programi/distribucija-regulacija-zraka/ (25. 10. 2014)

[5] **F. Rihl,** *Načrtovanje sistema prezračevanja in klimatizacije v poslovni stavbi*, master's thesis, 2015

Nomenclature

(Symbols)	(Symbol meaning)
TEB	Thermoelectric power plant Brestanica
DHW	domestic hot water
SV	fresh air
T	thermometer
KM	mixing chamber
H	hydrostat
F	filter
V2	fan for air extraction
PG	preheater
OdV	used air
HL	cooler
OtV	exhaust air
MK	chamber for air humidification

Žrv	grate of the recycled air
DG	heater
Žsv	grate of the fresh air
V1	fan for air supply
Žov	grate of the used air
PV	conditioned air
DP	differential pressure switch
UV	supply air in the area
RV	recycled air
$\dot{Q}_{HL}$	transmission heat losses [W]
$\dot{Q}_{T}$	heat flux [W]
ΔT	temperature difference [K]
$\dot{Q}_{p}$	heat gains due to people presence [W]
$\dot{Q}_{p_{tr}}$	sensitive heat [W]
$\dot{Q}_{p_{l}}$	latent heat [W]
N	number of people
$\dot{Q}_{M}$	heat of the devices and lighting [W]
A_{u}	usable area [m²]
$\dot{Q}_{S}$	solar radiation gains [W]
A_{i}	glass surface of the window [m²]
I_{max}	global solar radiation [W/m²]
A	total surface of the window [m²]
I_{difmax}	diffuse solar radiation [W/m²]
b	transmittance
s_{a}	the coefficient of accumulation
A_{PK}	cross-section of the duct [m²]
$\dot{V}$	volume air flow [m²/h]
w	air velocity [m/s]
A_{ef2}	effective surfice of protective grating [m²]

$B1$	width of protective grating [m]
$H1$	height of protective grating [m]
n	number of lamells
Δp	total pressure drop [Pa]
Δp_{lin}	linear pressure drop [Pa]
ε	the coefficient of the material roughness
ρ	density of the medium [kg/m^3]
d_H	hydraulic diameter [m]
L	length of the duct [m]
a, b	dimensions of the duct[m]
Δp_{lok}	local pressure drop [Pa]
ζ	the coefficient of the local resistance

Inštitut za energetiko Institute of Energy Technology

On December 2015, the Faculty of Energy Technologies of the University of Maribor completed the project to provide additional research infrastructure at the Institute of Energy, which include €4 million of research equipment in addition to the expanded facilities.

The Faculty of Energy Technologies of the University of Maribor is situated in Krško and has a separate department in Velenje. The faculty is active at Slovenia's two largest power stations: the Šoštanj Thermal Power Plant and the Krško Nuclear Power Plant. Furthermore, in addition to these two environments, it is directly or indirectly active in very large enterprise production and service activities throughout the energy sector. The integration of both local communities with energy technologies represents a great added value to studying at the faculty: students have the opportunity to encounter various energy systems in practice, and their acquired theoretical knowledge is thus further consolidated.

new photovoltaic field at the Institute of Energy Technology

Additional research infrastructure within the institute is a great asset to the faculty. It is possible to carry out research in the field of aero and hydro energy technologies, thermo-mechanics and thermal-energy, monitoring the efficiency of energy conversion, highly efficient electrical machines and drives, electric vehicles and vessels, the materials and their applied use of energy self-sufficient and smart electricity networks, detecting the potential of renewable energy sources, computer-supported prototypes design, and more.

3D visualisation system

Additional research capacity enables the implementation of interdisciplinary research with an emphasis on excellence. In the context of basic and applied research and the implementation of new knowledge, new products, processes and services that increase competitiveness of the economy are created.

The aforementioned equipment is a great asset for students of the faculty. A significant proportion of study at the Faculty of Energy Technologies is carried out in laboratories with up-to-date research equipment that provides excellent conditions for the acquisition of the applicable knowledge of students. Students with new equipment are enabled to have contact with state-of-the-art technology in the very broad field of energy, which is an important added value that students gain when entering the labour market.

according to survey 90% of all graduates are employed

The results of a survey confirmed that the students of the Faculty of Energy Technologies are well received by the labour market in terms of the employability of graduates and competencies acquired during their studies.

A total of 90% of all students who participated in the survey and who did not continue their studies at a higher level programs have a regular employment; 87% are active directly in the field of energy technologies.

Only 4.9% all graduates from the first generation of students who completed the study are reported as jobseekers at the Employment Service Institute, which is very encouraging.

In addition to companies engaged in electricity generation, transmission, managing and trading energy and maintaining of energy systems, the students of energy technologies are also valued by the companies that are aware of the importance of the rational use of energy and the associated impacts on operating costs.

Information on employment opportunities after the end of the studies is one of the main criteria on which young people decide on the type of study.

Study at the Faculty of Energy Technologies is therefore the right choice for all who want to good employment opportunities after graduation, as well as for those who wish to upgrade their knowledge and to obtain higher education. The faculty offers a friendly study environment and full study support from the freshman year to completion of one's doctoral thesis.

REPUBLIKA SLOVENIJA
MINISTRSTVO ZA IZOBRAŽEVANJE, ZNANOST IN ŠPORT

Univerza v Mariboru
Fakulteta za energetiko

Naložba v vašo prihodnost
OPERACIJO DELNO FINANCIRA EVROPSKA UNIJA
Evropski sklad za regionalni razvoj

»Operacijo delno financira Evropska unija, in sicer iz Evropskega sklada za regionalni razvoj ter Ministrstvo za izobraževanje, znanost in šport. Operacija se izvaja v okviru Operativnega programa krepitve regionalnih razvojnih potencialov za obdobje 2007-2013, razvojne prioritete: Gospodarsko-razvojna infrastruktura, prednostne usmeritve Izobraževalno-raziskovalna infrastruktura.«

MAIN TITLE OF THE PAPER
SLOVENIAN TITLE

Author[1], Author [2], Corresponding author[✉]

Keywords: (Up to 10 keywords)

Abstract

Abstract should be up to 500 words long, with no pictures, photos, equations, tables, only text.

Povzetek

(Abstract in Slovenian language)

Submission of Manuscripts: All manuscripts must be submitted in English by e-mail to the editorial office at jet@um.si to ensure fast processing. Instructions for authors are also available online at http://www.fe.um.si/en/jet/author-instructions.html.

Preparation of manuscripts: Manuscripts must be typed in English in prescribed journal form (MS Word editor). A MS Word template is available at the Journal Home page.

A title page consists of the main title in the English and Slovenian language; the author(s) name(s) as well as the address, affiliation, E-mail address, telephone and fax numbers of author(s). Corresponding author must be indicated.

Main title: should be centred and written with capital letters (ARIAL bold 18 pt), in first paragraph in English language, in second paragraph in Slovenian language.

Key words: A list of 3 up to 6 key words is essential for indexing purposes. (CALIBRI 10pt)

Abstract: Abstract should be up to 500 words long, with no pictures, photos, equations, tables, - text only.

Povzetek: - Abstract in Slovenian language.

✉ Corresponding author: Title, Name and Surname, Tel.: +XXX x xxx xxx, Mailing address: xxxxxxxxxxxxxxxxxxxxxxxxxxxxxxxxx, E-mail address: x.x@xxx.xx

[1] Organisation, Department, Address

[2] Organisation, Department, Address

[3] Organisation, Department, Address

Main text should be structured logically in chapters, sections and sub-sections. Type of letters is Calibri, 10pt, full justified.

Units and abbreviations: Required are SI units. Abbreviations must be given in text when first mentioned.

Proofreading: The proof will be send by e-mail to the corresponding author in MS Word's Track changes function. Corresponding author is required to make their proof corrections with accepting or rejecting the tracked changes in document and answer all open comments of proof reader. The corresponding author is responsible to introduce corrections of data in the paper. The Editors are not responsible for damage or loss of submitted text. Contributors are advised to keep copies of their texts, illustrations and all other materials.

The statements, opinions and data contained in this publication are solely those of the individual authors and not of the publisher and the Editors. Neither the publisher nor the Editors can accept any legal responsibility for errors that could appear during the process.

Copyright: Submissions of a publication article implies transfer of the copyright from the author(s) to the publisher upon acceptance of the paper. Accepted papers become the permanent property of "Journal of Energy Technology". All articles published in this journal are protected by copyright, which covers the exclusive rights to reproduce and distribute the article as well as all translation rights. No material can be published without written permission of the publisher.

Chapter examples:

1 MAIN CHAPTER

(Arial bold, 12pt, after paragraph 6pt space)

1.1 Section

(Arial bold, 11pt, after paragraph 6pt space)

1.1.1 Sub-section

(Arial bold, 10pt, after paragraph 6pt space)

Example of Equation (lined 2 cm from left margin, equation number in normal brackets (section. equation number), lined right margin, paragraph space 6pt before in after line):

Equation (1.1)

Tables should have a legend that includes the title of the table at the top of the table. Each table should be cited in the text.

Table legend example:

Table 1: *Name of the table (centred, on top of the table)*

Figures and images should be labelled sequentially numbered (Arabic numbers) and cited in the text – Fig.1 or Figure 1. The legend should be below the image, picture, photo or drawing.

Figure legend example:

Figure 1: *Name of the figure (centred, on bottom of figure, photo, or drawing)*

References

[1] **N. Surname:** Title, Publisher or Journal Title, Vol., Iss., p.p., Year of Publication

Examples:

[2] **J. Usenik:** Mathematical model of the power supply system control, Journal of Energy Technology, Vol. 2, Iss. 3, p.p. 29 – 46, 2009

[3] **J.J. DiStefano, A.R. Stubberud, I.J.Williams:** Theory and Problems of Feedback and Control Systems, McGraw-Hill Book Company, 1987

Example of reference-1 citation: In text [1], text continue.

Nomenclature

(Symbols)	(Symbol meaning)
t	time

JET

ISSN 1855-5748

JET I Journal of Energy Technology I Vol. 8, Issue 4, December 2015 I University of Maribor, Faculty of Energy Technology